Electronic Supplementary Information (ESI)

Emission behaviors of novel V- and X-shaped fluorophores in response to pH and force stimuli

Hong-Yu Fu, Ning Xu, Yi-Min Pan, Xiao-Lin Lu and Min Xia*

Department of Chemistry, Zhejiang Sci-Tech University, Hangzhou 310018, P. R. China

E-mail: xiamin@zstu.edu.cn

Materials and measurements

All the reagents were analytically pure and some chemicals were further purified by recrystallization or distillation. Melting points were determined by an OptiMelt automated melting point system. The ^{1}H NMR (400 MHz) and ^{13}C NMR (100 MHz) spectra were obtained on a Bruker Avance II DMX 400 spectrometer with $CDCl_3$ or DMSO-d_6 as the solvent. The absorption spectra were measured on a Shimadzu UV 2501(PC)S UV–Vis spectrometer, and the fluorescence spectra were acquired on a Perkin-Elmer LS55 spectrophotometer. The quantum yields were measured with quinine sulfate in 0.1 M sulfuric acid solution (Φ_f =0.55) as the reference and the solid-state quantum yields were gained by an integral sphere. The mass spectrum was recorded on a HP 1110 mass spectrometer. The crystallographic data were determined on a Bruker Gemini Ultra diffractometer with a CCD counter. The powder X-ray diffraction patterns were recorded on DX2700 with Cu-K_α radiation operating at 40 kV and 40 mA by a 0.3°/min scanning rate. TOF-MS was measured on a Waters Xevo G_2-S mass spectrometer. Dynamic light scattering is carried out on a Beckman Coulter particle analyzer with 50 μM aggregate in MeCN/H_2O mixture (5 : 95, v/v) at 25 °C. 2, 5-dibromoterephthalaldehyde was prepared according to the reported method [1].

Synthesis of intermediates (1-1) or (1-2)

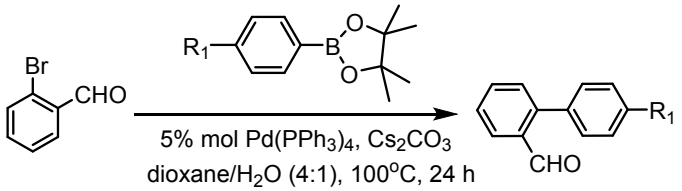

1-1 [R_1= OCH_3]
1-2 [R_2= $N(CH_3)_2$]

At room temperature and N_2 flux, the solution of *N, N*-dimethyl-4-(4,4,5,5-tetramethyl-1,3,2-dioxaborolan-2-yl)aniline (12 mmol, 2.95 g) or 2-(4-methoxyphenyl)-4,4,5,5-tetramethyl-1,3,2-dioxa borolane (12 mmol, 2.80 g) in dioxane/H_2O (4:1, v/v, 20 mL) was injected into the mixture of 2-bromo-benzaldehyde (10 mmol, 1.83 g), $Pd(PPh_3)_4$ (0.5 mmol, 0.577 g) and $CsCO_3$(15 mmol, 2.89 g) in dioxane/H_2O (4:1, v/v, 30 mL). The resulted mixture was heated at 100°C for 24 h and then cooled to room temperature. After filtration, the filtrate was diluted with water and extracted by CH_2Cl_2 (2×15 mL).

The combined organic layers were dried over anhydrous Na_2SO_4. After the removal of solvent, the residue was purified on a silica gel column chromatography.

4'-(methyloxyl)-[1,1'-biphenyl]-2-carbaldehyde (1-1): 94% yield; m.p. 52.8-54.2°C; ^{1}H NMR(400MHz, $CDCl_3$) δ 3.87(s, 3H), 6.70(d, *J*=8.4 Hz, 2H), 7.30(d, *J*=8.4 Hz), 7.42-7.47(m, 2H), 7.61(t, *J*=7.6 Hz), 9.99(s, 1H); ^{13}C NMR(100MHz, $CDCl_3$) δ 55.40, 113.96, 127.38, 127.62, 130.04, 130.79, 131.31, 133.52, 133.79, 145.44, 159.73, 192.69; EI-MS (70eV) *m/z* (%) 212(M^+, 100), 197(45), 181(57), 169(88), 152(36), 141(100), 128(16), 115(93), 89(16), 63(15).

4'-(dimethylamino)-[1,1'-biphenyl]-2-carbaldehyde (1-2): 88% yield; m.p. 77.4-79.3°C; ^{1}H NMR (400MHz, $CDCl_3$) δ 2.93(s, 6H), 6.71(d, *J*=7.6 Hz, 2H), 7.17(d, *J*=8.0Hz, 2H), 7.31-7.37(m, 2H), 7.50(t, *J*=7.6Hz, 1H), 7.79(d, *J*=8.0Hz, 1H), 9.94(s, 1H); ^{13}C NMR(100MHz, $CDCl_3$) δ 40.58, 112.05, 126.63, 127.54, 130.63, 131.10, 133.42, 133.61, 146.30, 150.26, 193.54; EI-MS (70eV) *m/z* (%) 225(M^+, 100), 196(45), 182(29), 167(12), 152(49), 141(13), 128(17), 115(17), 69(23), 51 (25), 42(47).

Synthesis of intermediates (2-1) or (2-2)

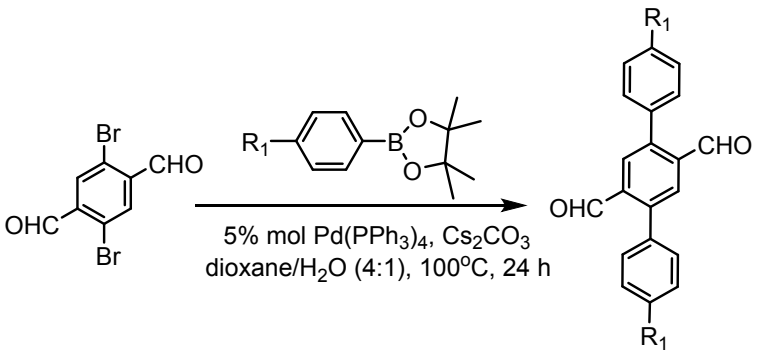

2-1 [R_1= OCH_3]
2-2 [R_2= $N(CH_3)_2$]

At room temperature and N_2 flux, the solution of *N, N*-dimethyl-4-(4,4,5,5-tetramethyl-1,3,2-dioxaborolan-2-yl)aniline (24 mmol, 5.90 g) or 2-(4-methoxyphenyl)-4,4,5,5-tetramethyl-1,3,2-dioxaborolane (24 mmol, 5.60 g) in dioxane/H_2O (4:1, v/v, 30 mL) was injected into the mixture of 2,5-dibromo-terephthalaldehyde (10 mmol, 2.98g), $Pd(PPh_3)_4$ (0.5 mmol, 0.577 g) and $CsCO_3$(30 mmol, 5.78 g) in dioxane/H_2O (4:1, v/v, 30 mL). The resulted mixture was heated at 100°C for 24 h and then cooled to room temperature. After filtration, the filtrate was diluted with water and extracted by CH_2Cl_2 (3×15 mL). The combined organic layers were dried over anhydrous Na_2SO_4. After the removal of solvent, the residue was purified on a silica gel column chromatography.

4,4''-dimethoxy-[1,1':4',1''-terphenyl]-2',5'-dicarbaldehyde (**2-1**): 83% yield; m.p. 189.2-191.0 °C; ^{1}H NMR (400MHz, $CDCl_3$) δ 3.89(s, 6H), 7.04(d, *J*=8.4 Hz, 4H), 7.36(d, *J*=8.4 Hz, 4H), 8.06(s, 2H), 10.08(s, 2H); ^{13}C NMR(100MHz, $CDCl_3$) δ 55.44, 114.14, 128.73, 130.14, 131.31, 136.36, 143.79, 160.08, 192.31; EI-MS (70eV) *m/z* (%) 346(M^+, 100), 232(18), 202(30), 139(20).

4,4''-bis(dimethylamino)-[1,1':4',1''-terphenyl]-2',5'-dicarbaldehyde (2-2): 80% yield; m.p. 238.4-240.1 °C; ^{1}H NMR(400MHz, $CDCl_3$) δ 3.04(s, 12H), 6.82(d, *J*=8.0 Hz, 4H), 7.31(d, *J*=8.0 Hz, 4H), 8.06(s, 2H), 10.10(s, 2H); ^{13}C NMR (100MHz, $CDCl_3$) δ 40.36, 112.18, 124.05, 129.92, 131.10, 136.40, 143.67, 150.49, 192.86; EI-MS (70eV) *m/z* (%) 372(M^+, 100), 315(30), 120(16), 69(14), 42(18).

Synthesis of V-shaped compounds (V_1-V_4)

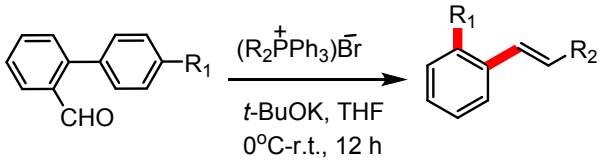

V_1-V_4

At 0°C and N_2 flux, *t*-BuOK (10 mmol) was added into the corresponding triphenyl phosphonium bromide (10 mmol) in dried THF (20 mL), the mixture was stirred for 30 min. The solution of compound **1-1** or **1-2** (8 mmol) in dried THF (10 mL) was injected into the above mixture. The resulted mixture was kept at the same temperature for 1 h and stirred at room temperature for 12 h. After poured into water, the mixture was extracted with ethyl acetate (2×15 mL). The combined organic layers were dried over anhydrous Na_2SO_4. After the removal of solvent, the residue was purified on a silica gel column chromatography.

(*E*)-2-(2-(4'-methoxy-[1,1'-biphenyl]-2-yl)vinyl)benzo[d]thiazole (**V_1**): 89% yield; m.p. 101.3-102.9 °C;

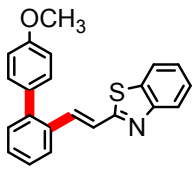

V_1

^{1}H NMR(400MHz, $CDCl_3$) δ 3.88(s, 3H), 7.00(d, *J*=8.4 Hz, 2H), 7.31-7.46(m, 8H), 7.52(d, *J*=16.4 Hz, 1H), 7.78(d, *J*=8.0 Hz, 2H), 7.97(d, *J*=8.0 Hz, 1H); ^{13}C NMR (100MHz, $CDCl_3$) δ 55.36, 113.77, 121.43, 122.92, 125.34, 126.26, 126.41, 127.47, 129.28, 130.46, 131.11, 132.46, 133.51, 134.27, 137.63, 141.83, 153.79, 159.19, 167.62; EI-MS (70eV) *m/z* (%) 343(M$^+$, 63), 312(42), 298(16), 236(31), 208(100), 195(17), 165(46), 109(7), 69(8).

(*E*)-N,N-dimethyl-2'-(2-(quinolin-2-yl)vinyl)-[1,1'-biphenyl]-4-amine (**V_2**): 84% yield; m.p. 139.8-141.2 °C; ^{1}H NMR(400MHz, $CDCl_3$) δ 3.02(3, 6H), 6.81(d, *J*=8.0 Hz, 2H), 7.31-7.48(m, 7H), 7.57(d, *J*=8.8 Hz, 1H), 7.62-7.70(m, 2H), 7.74(d, *J*=8.0 Hz, 1H), 7.87(m, 1H), 8.04(t, *J*=8.8 Hz, 2H); ^{13}C NMR (100MHz, $CDCl_3$) δ 39.57, 111.08, 117.42, 125.04, 125.43, 125.81, 126.14, 126.40, 127.44, 127.51, 128.04, 128.62, 129.25, 129.81, 133.43, 133.57, 135.18, 141.01, 147.07, 148.68, 155.72; EI-MS (70eV) *m/z* (%) 350(M$^+$, 100), 335(15), 306(16), 221(39), 208(14), 178(14), 165(12), 143(11), 130(37), 102(8), 77(6).

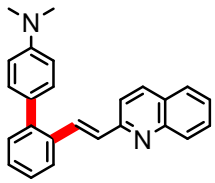

V_2

(*E*)-2'-(2-(benzo[d]thiazol-2-yl)vinyl)-N,N-dimethyl-[1,1'-biphenyl]-4-amine (**V_3**): 73% yield; m.p. 114.9-116.3°C; ^{1}H NMR(400MHz, $CDCl_3$) δ 3.03(s, 6H), 6.83(d, *J*=8.8Hz, 2H), 7.29-7.47(m, 8H), 7.62(d, *J*=16Hz, 1H), 7.78(m, 2H), 7.98(d, *J*=8.0Hz, 1H); ^{13}C NMR (100MHz, $CDCl_3$) δ 40.51, 112.13, 121.38, 121.70, 122.57, 122.86, 123.61, 125.19, 126.15, 126.45, 126.85, 129.16, 130.34, 130.83, 133.34, 134.30, 138.21, 142.32, 153.88, 167.89; EI-MS (70eV) *m/z* (%) 356(M$^+$, 57), 310(11), 236(22), 221(100), 178(24), 108(12), 69(21), 42(12).

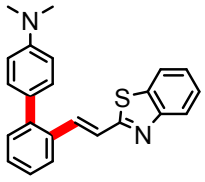

V_3

(*E*)-2-(2-(4'-methoxy-[1,1'-biphenyl]-2-yl)vinyl)quinoline (**V_4**): 76% yield, yellowish oil; ^{1}H NMR (400MHz, $CDCl_3$) δ 3.87(s, 3H), 6.99(d, *J*=8.8 Hz, 2H), 7.34-7.42(m, 6H), 7.46(t, *J*=8 Hz, 1H), 7.51(d, *J*=8.8 Hz, 1H), 7.61(d, *J*=16.4Hz, 1H), 7.73(d, *J*=8 Hz, 1H), 7.88(m, 1H), 8.03(m, 1H); ^{13}C NMR (100MHz, $CDCl_3$) δ 55.36, 113.67, 118.50, 126.19, 126.40, 127.23, 127.42, 127.48, 128.50, 129.12, 129.73, 130.02, 130.38, 131.14, 133.06, 133.96, 134.59, 136.31, 141.51,

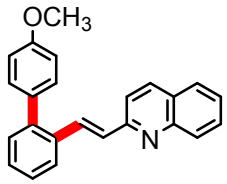

V_4

148.12, 156.52, 159.00; EI-MS (70eV) *m/z* (%) 337(M^+, 100), 322(34), 306(83), 292(22), 230(12), 165(19), 129(54).

Synthesis of X-shaped compounds (X_1-X_2)

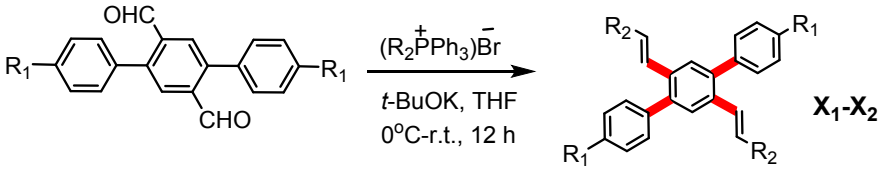

At 0°C and N_2 flux, *t*-BuOK (22 mmol) was added into the corresponding triphenyl phosphonium bromide (22 mmol) in dried THF (30 mL), the mixture was stirred for 30 min. The solution of compound **2-1** or **2-2** (10 mmol) in dried THF (10 mL) was injected into the above mixture. The resulted mixture was kept at the same temperature for 1 h and stirred at room temperature for 12 h. The formed precipitate was collected and washed with ethanol for 2-3 times. The solid was pure enough for spectral analysis.

2,2'-((1*E*,1'*E*)-(4,4''-dimethoxy-[1,1':4',1''-terphenyl]-2',5'-diyl)bis(ethene-2,1-diyl))bis(benzo[d]-thiazole) (**X_1**): 63% yield; m.p. 326.7-328.3 °C; ^{1}H NMR(400MHz, $CDCl_3$) δ 3.93(s, 6H), 7.06(d, *J*=8.0 Hz, 4H), 7.34-7.49(m, 10H), 7.58(d, *J*=16.0 Hz, 2H), 7.81(m, 4H), 7.98(d, *J*=8.0 Hz, 2H); ^{13}C NMR (100MHz, $CDCl_3$) δ 55.67, 114.31, 121.66, 123.22, 123.87, 125.62, 126.59, 128.66, 131.38, 131.92, 134.54, 134.68, 137.01, 141.09, 154.24, 159.70, 167.38; TOF-MS *m/z* (%) 623.31(M^+, 100).

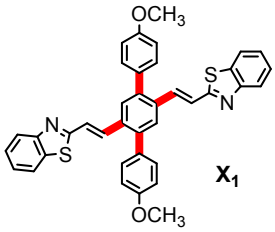

X_1

2',5'-bis((*E*)-2-(isoquinolin-3-yl)vinyl)-N4,N4,N4'',N4''-tetramethyl-[1,1':4',1''-terphenyl]-4,4''-diamine (**X_2**): 54% yield; m.p. 342.1-343.7°C; ^{1}H NMR(400MHz, $CDCl_3$) δ 3.06(s, 12H), 6.87(d, *J*=8.4 Hz, 4H), 7.42-7.51(m, 8H), 7.61(d, *J*=8.8 Hz, 2H), 7.68(t, *J*=8.0 Hz, 2H), 7.74-7.78(m, 4H), 7.92(s, 2H), 8.04(dd, J_1=8.4 Hz, J_2=3.2 Hz, 4H); TOF-MS *m/z* (%) 609.16(M^+, 100).

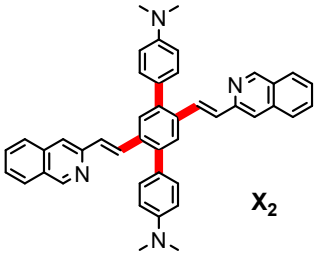

X_2

X-ray structure analysis

A single crystal of the title compound grown in EtOH-MeCN mixture (7:3, v/v) was selected for the X-ray analysis. The diffraction data were collected on a Bruker CCD area-detector diffractometer equipped with a graphite-monochromated Mo*Ka* radiation (λ=0.71073 Å). The unit cell parameters were determined from a least-squares refinement of the setting angles. The structure was solved by direct methods and refined on F^2 by the full-matrix least-squares methods with SHELXS-97. The refinement was carried out by full-matrix least squares method on the positional and anisotropic temperature parameters of the non-hydrogen atoms using SHELXL-97. All H atoms were placed in the idealized positions and constrained to ride on their parent atoms. Compound **V_2**: $C_{25}H_{22}N_2$, M_w = 350.45, triclinic, *a* = 8.1532(5) Å, *b* = 10.2921(7) Å, *c* = 12.9838(11) Å, *α* = 66.763(7) °, *β* = 88.564(6) °, *γ* = 73.285(6) °, D_{calcud} = 1.220 g cm^{-3}, *Z* = 2, *F(000)* = 372, *μ* = 0.547mm^{-1}, 3767 reflections were corrected, 3648 unique, R_1 = 0.0456, wR_2 = 0.1268. Compound **V_3**: $C_{23}H_{20}N_2S$, M_w = 356.47, monoclinic, *a* = 12.5537(8)

Å, b = 6.3103(4) Å, c = 23.6534(17) Å, α = 90 °, β = 99.738(6)°, γ = 90°, D_{calcud} = 1.282 g cm^{-3}, Z = 4, $F(000)$ = 752, μ = 0.184 mm^{-1}, 3389 reflections were corrected, 3377 unique, R_1 = 0.0437, wR_2 = 0.1125. Crystallographic data for compound **V_2** (CCDC 1521255) and **V_3** (CCDC 1480706) were deposited at CCDC center and can be obtained free of charge from The Cambridge Crystallographic Data Centre via www.ccdc.cam.ac.uk/data_ request/cif.

Computational method

The gas-phase geometries of the concerned compounds were optimized without any symmetry restrictions in singlet ground state using the density functional theory (DFT) method at the B3LYP level. The 6-31G (d, p) basis set was selected for all the elements. The vibration frequency calculations were performed to ensure that the optimized geometries represented the global minima on the ground-state potential energy surface. All the calculations were carried out with the Gaussian 09 program package in aid of the GaussView visualization program [2].

References:

[1] X. Yang, D. Liu and Q. Miao, *Angew. Chem. Int. Ed.*, 2014, **53**, 6786-6790.

[2] M. J. Frisch, G. W. Trucks, H. B. Schlegel, G. E. Scuseria, M. A. Robb, J. R. Cheeseman, G. Scalmani, V. Barone, B. Mennucci, G. A. Petersson, H. Nakatsuji, M. Caricato, X. Li, H. P. Hratchian, A. F. Izmaylov, J. Bloino, G. Zheng, J. L. Sonnenberg, M. Hada, M. Ehara, K. Toyota, R. Fukuda, J. Hasegawa, M. Ishida, T. Nakajima, Y. Honda, O. Kitao, H. Nakai, T. Vreven, J. A. Montgomery, Jr., J. E. Peralta, F. Ogliaro, M. Bearpark, J. J. Heyd, E. Brothers, K. N. Kudin, V. N. Staroverov, R. Kobayashi, J. Normand, K. Raghavachari, A. Rendell, J. C. Burant, S. S. Iyengar, J. Tomasi, M. Cossi, N. Rega, J. M. Millam, M. Klene, J. E. Knox, J. B. Cross, V. Bakken, C. Adamo, J. Jaramillo, R. Gomperts, R. E. Stratmann, O. Yazyev, A. J. Austin, R. Cammi, C. Pomelli, J. W. Ochterski, R. L. Martin, K. Morokuma, V. G. Zakrzewski, G. A. Voth, P. Salvador, J. J. Dannenberg, S. Dapprich, A. D. Daniels, O. Farkas, J. B. Foresman, J. V. Ortiz, J. Cioslowski and D. J. Fox, Gaussian 09, Revision A.02, Gaussian, Inc., Wallingford CT, 2009.

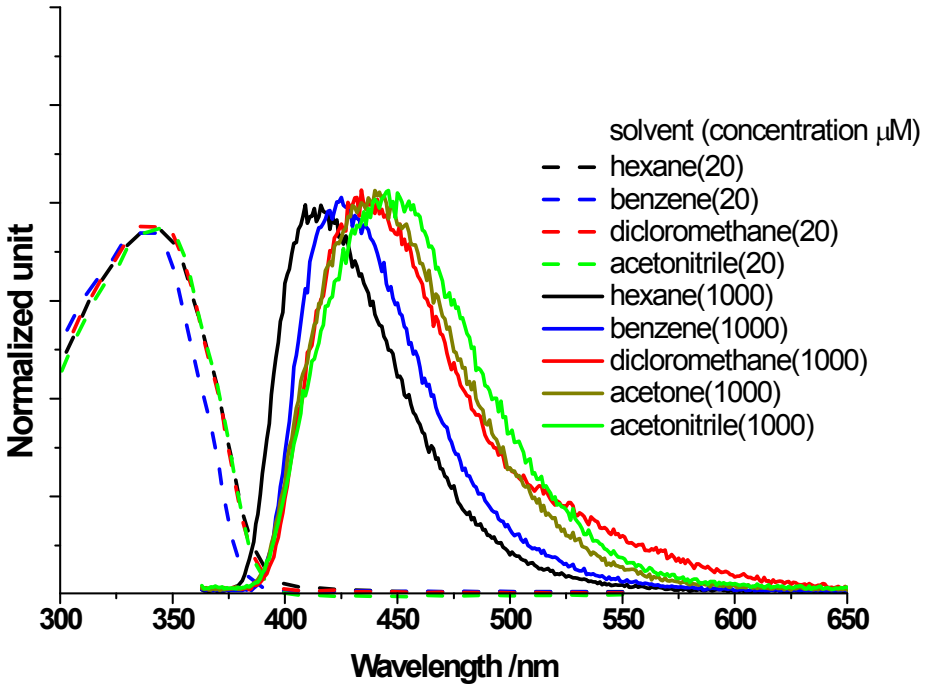

Fig. S1 Absorption (dash line) and emission spectra [solid line, λ_{ex} = 350 nm, slit width (ex, em) / nm : 5, 10] of $\mathbf{V_1}$ in different solvents

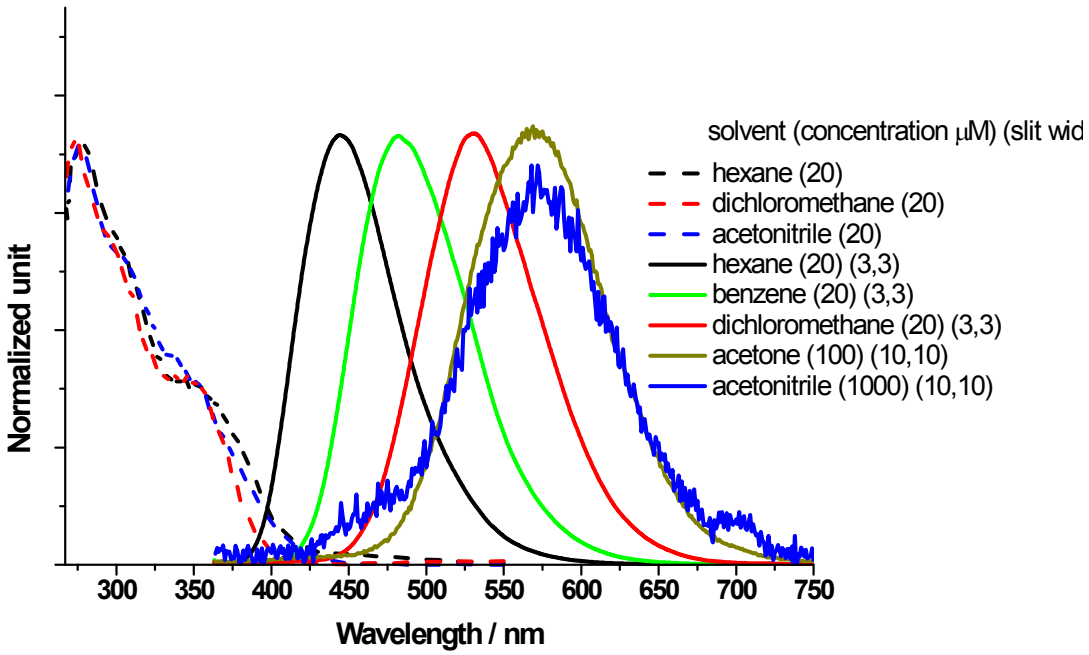

Fig. S2 Absorption (dash line) and emission spectra (solid line, λ_{ex} = 350 nm) of $\mathbf{V_2}$ in different solvents

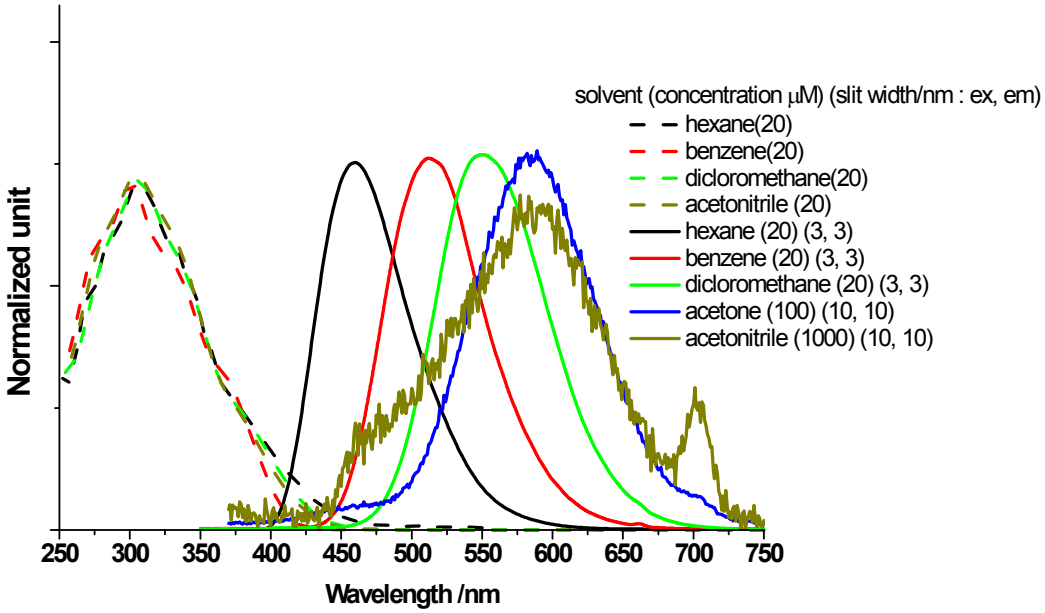

Fig. S3 Absorption (dash line) and emission spectra (solid line, λ_{ex} = 350 nm) of **V_3** in different solvents

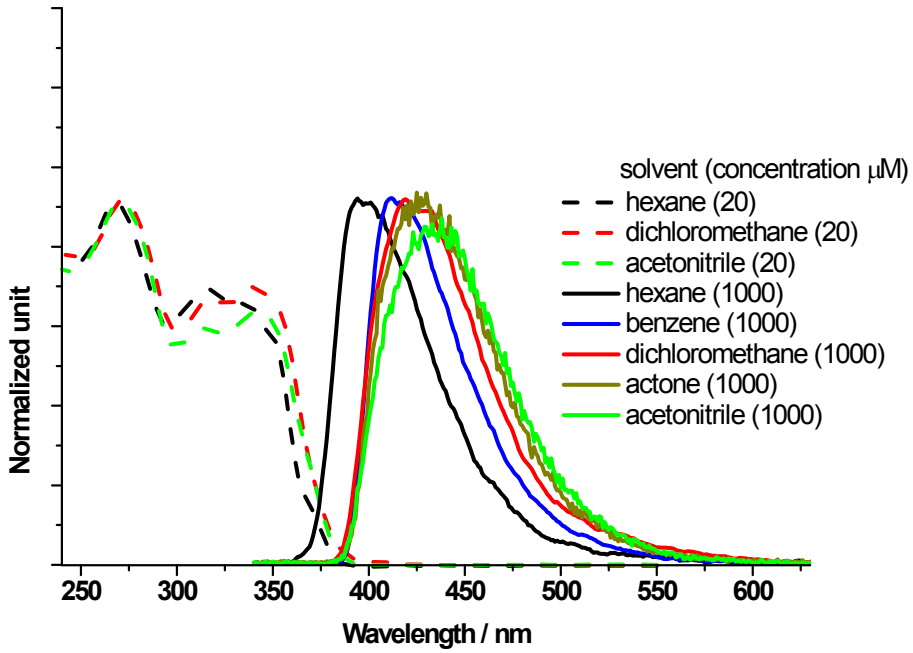

Fig. S4 Absorption (dash line) and emission spectra [solid line, λ_{ex} = 350 nm, slid width (ex, em) / nm : 5, 10] of **V_4** in different solvents

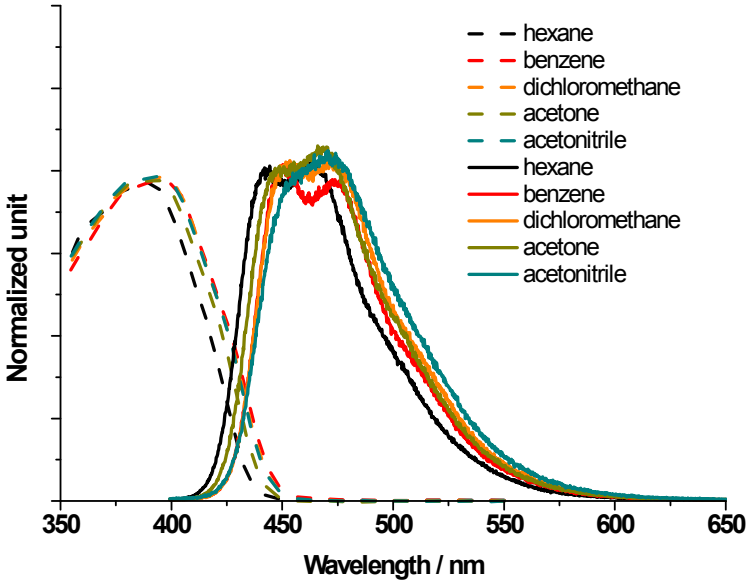

Fig. S5 Absorption (dash line, 10 μM) and emission spectra [solid line, 10 μM, λ_{ex} = 350 nm, slid width (ex, em) / nm : 5, 10] of $\mathbf{X_1}$ in different solvents

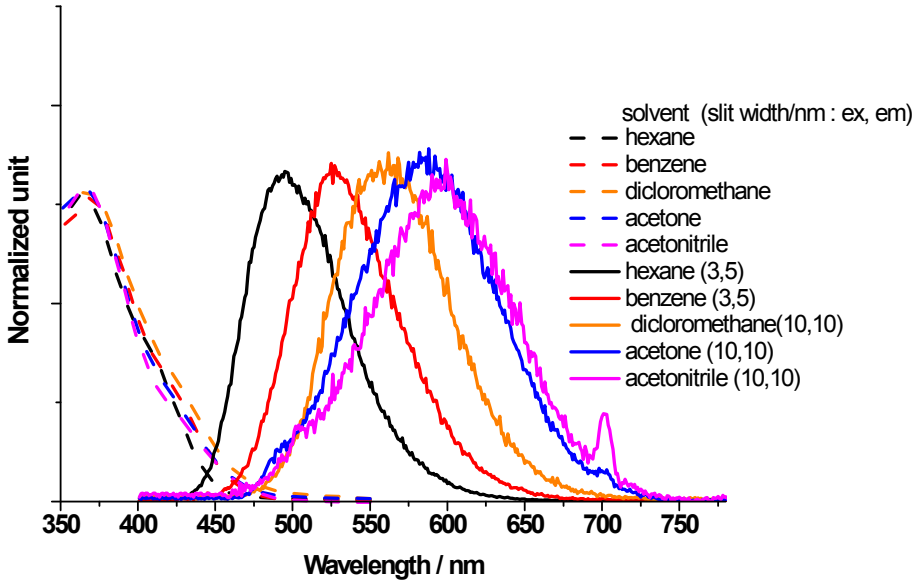

Fig. S6 Absorption (dash line, 10 μM) and emission spectra (solid line, 10 μM, λ_{ex} = 350 nm)

of $\mathbf{X_2}$ in different solvents

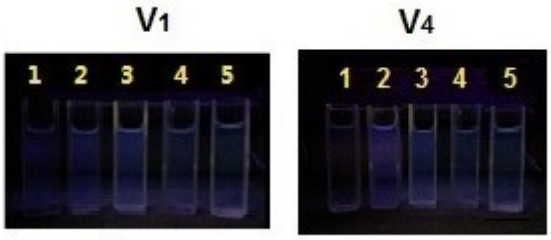

Fig. S7 Photos of $\mathbf{V_1}$ and $\mathbf{V_4}$ (50 μM) in different solvents under 365 nm UV light (1: *n*-hexane; 2: benzene; 3: CH_2Cl_2; 4: acetone; 5: MeCN);

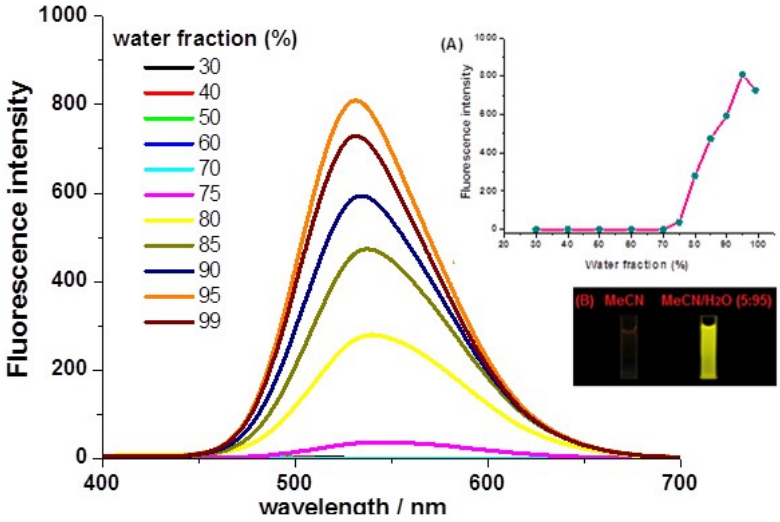

Fig. S8 Emission spectra of $\mathbf{V_3}$ (50 μM) in MeCN with varied water fraction [*inserted*: (A) the fluorescence intensity of $\mathbf{V_3}$ in MeCN with varied water fraction; (B) photos of $\mathbf{V_3}$ in MeCN and MeCN/ H_2O (v/v, 5:95) mixture]

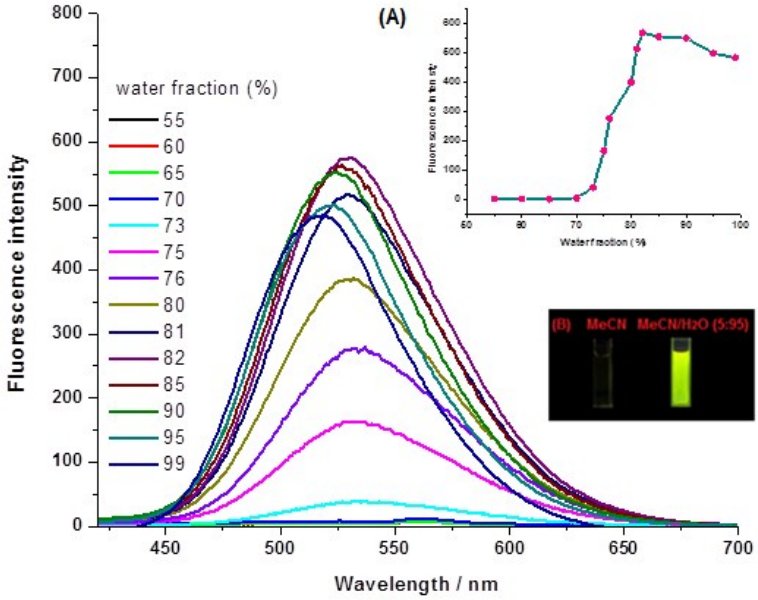

Fig. S9 Emission spectra of $\mathbf{V_2}$ (50 μM) in MeCN with varied water fraction [*inserted*: (A) the fluorescence intensity of $\mathbf{V_2}$ in MeCN with varied water fraction; (B) photos of $\mathbf{V_2}$ in MeCN and MeCN/H_2O (v/v, 5:95) mixture]

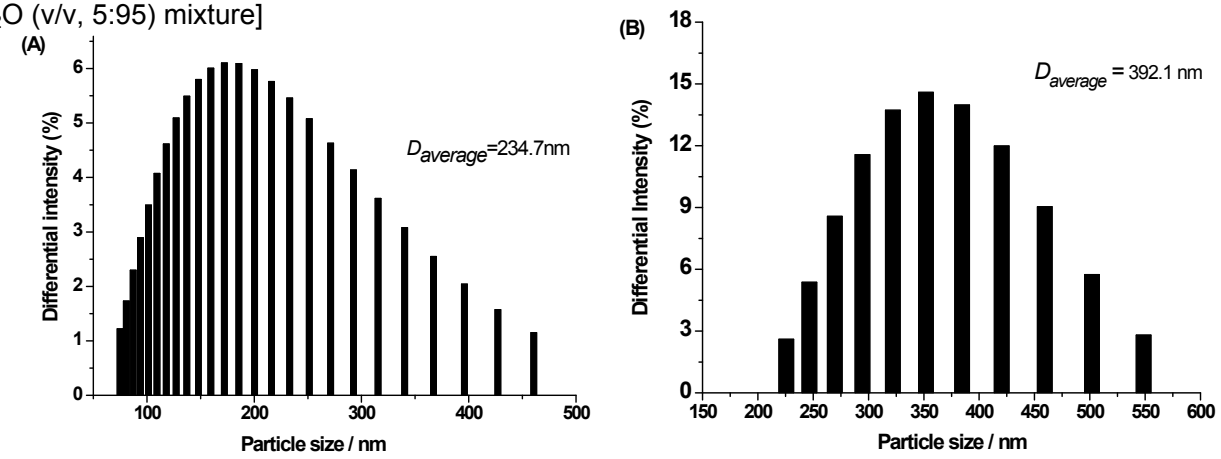

Fig. S10 Dynamic light scattering of $\mathbf{V_2}$ (A) and $\mathbf{V_3}$ (B) (50 μM) in MeCN/H_2O (5:95) mixture

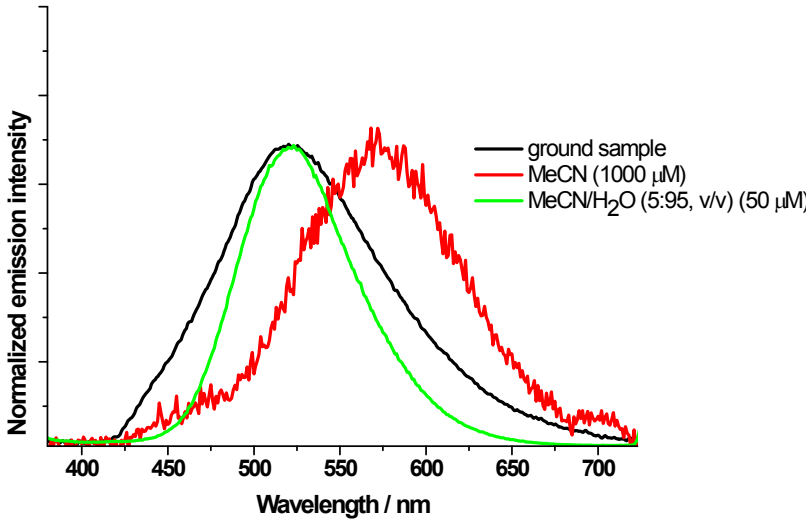

Fig. S11 Emission spectra (λ_{ex}= 350 nm) of $\mathbf{V_2}$ in MeCN solution, MeCN/H_2O (5:95) mixture and ground state

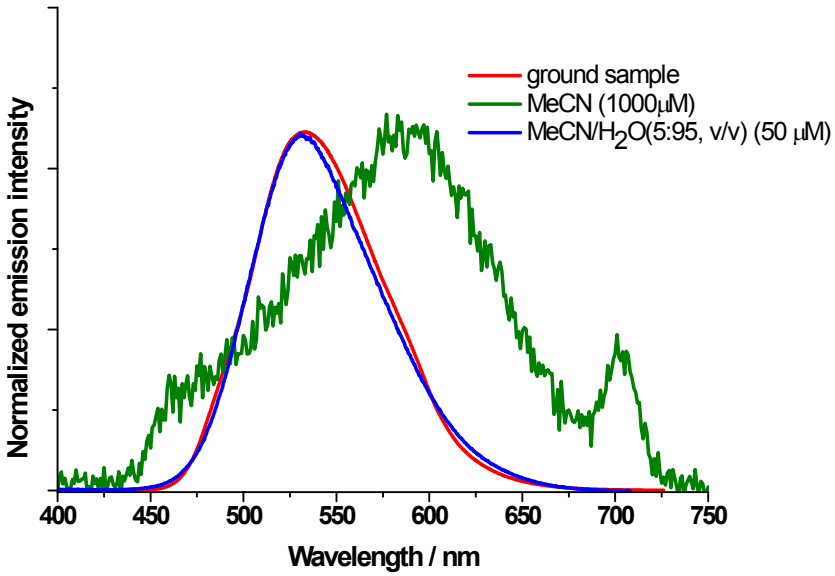

Fig. S12 Emission spectra (λ_{ex}= 350 nm) of $\mathbf{V_3}$ in MeCN solution, MeCN/H_2O (5:95) mixture and ground state

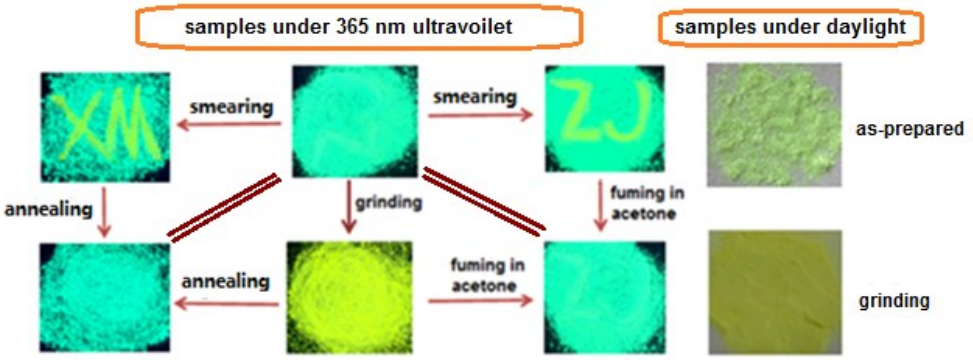

Fig. S13 Photos of compound $\mathbf{V_3}$ in solid state under daylight and 365 nm ultraviolet (smearing with a thin glass rod; annealing at 80°C for 2 min; fuming in acetone vapour for 2 min)

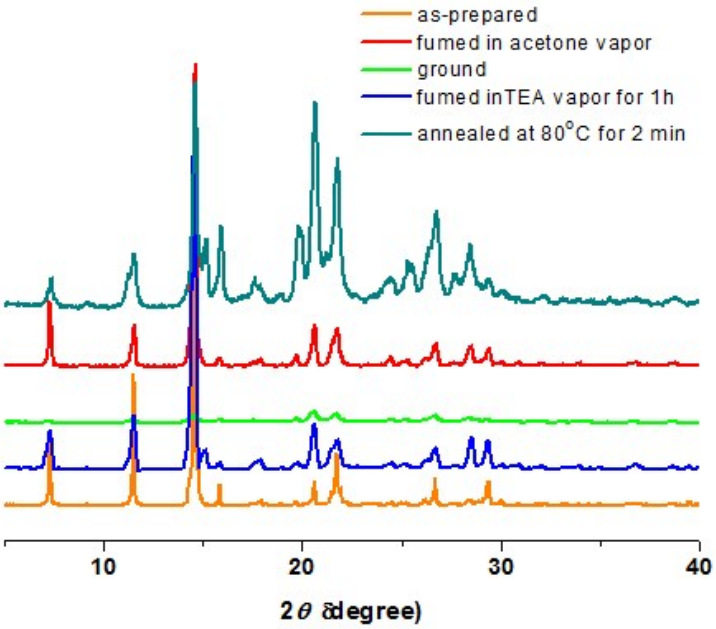

Fig. S14 PXRD patterns of compound $\mathbf{V_3}$ under different phases

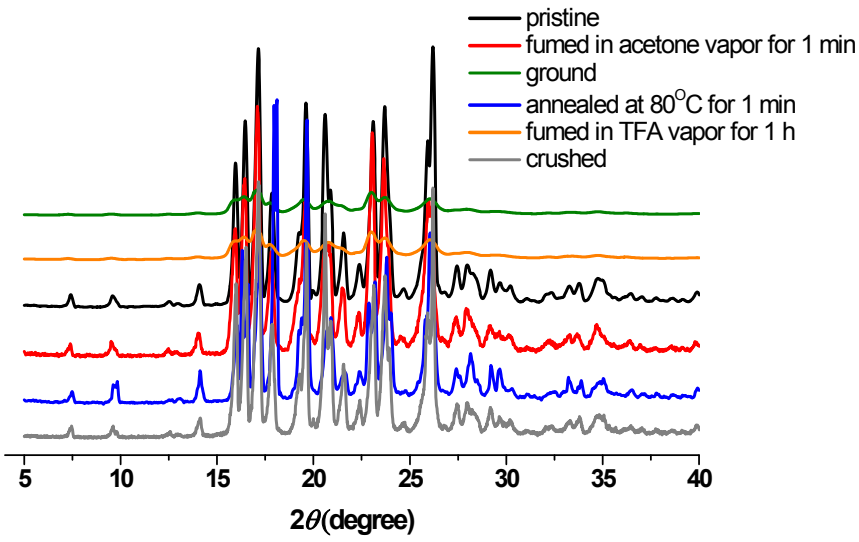

Fig. S15 PXRD patterns of compound $\mathbf{V_2}$ under different phases

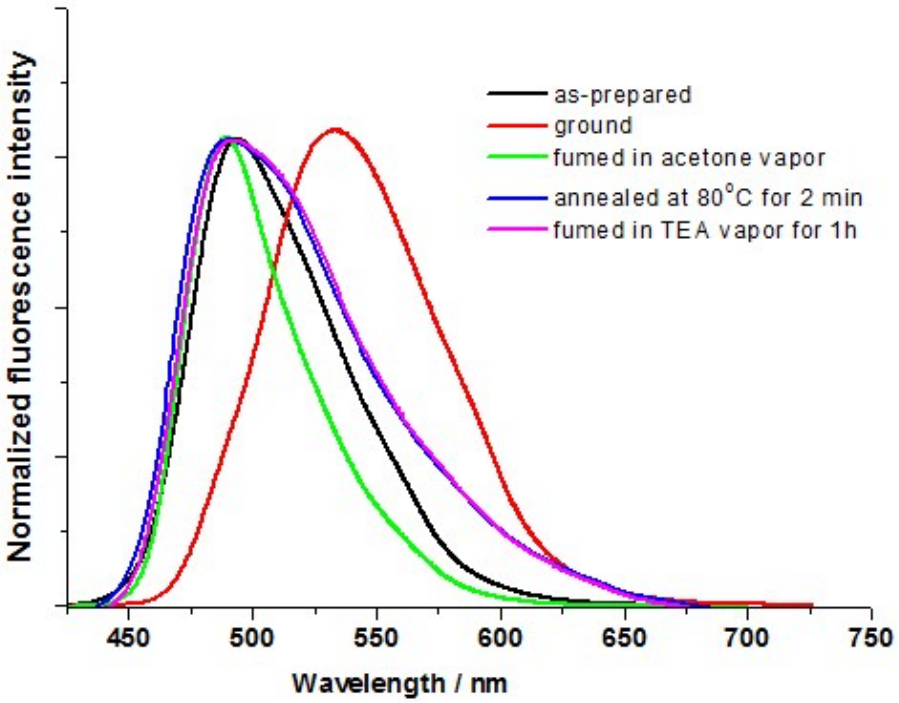

Fig. S16 Emission spectra of compound $\mathbf{V_3}$ under different solid phases

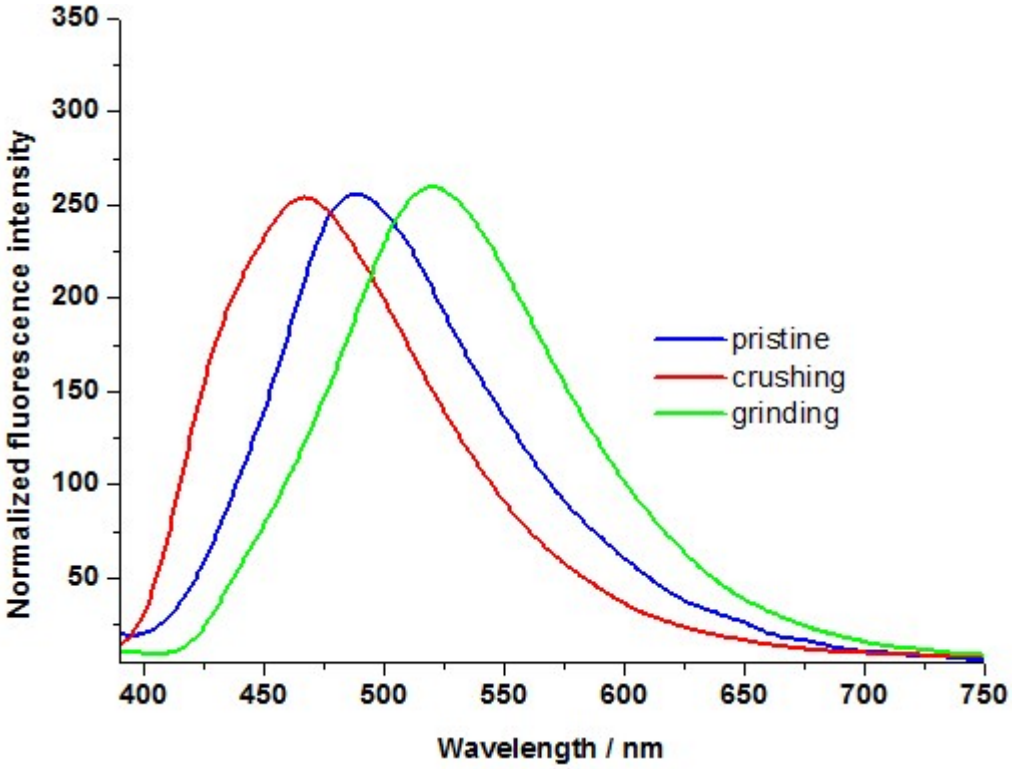

Fig. S17 Emission spectra of compound $\mathbf{V_2}$ under different solid phases

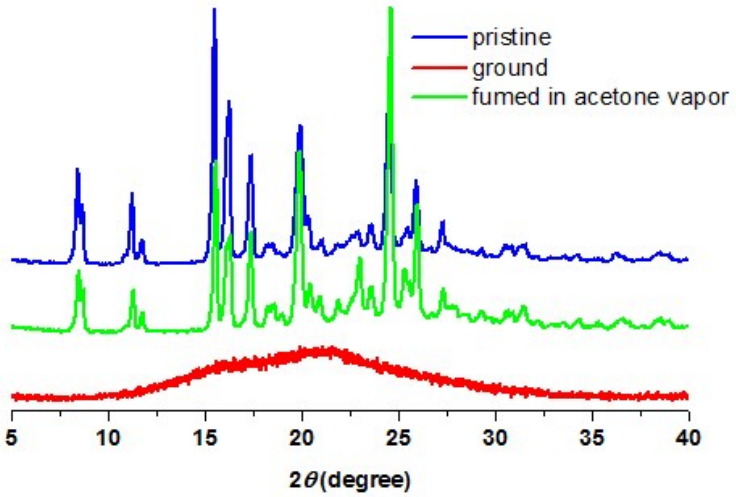

Fig. S18 PXRD patterns of compound $\mathbf{V_1}$ under different phases

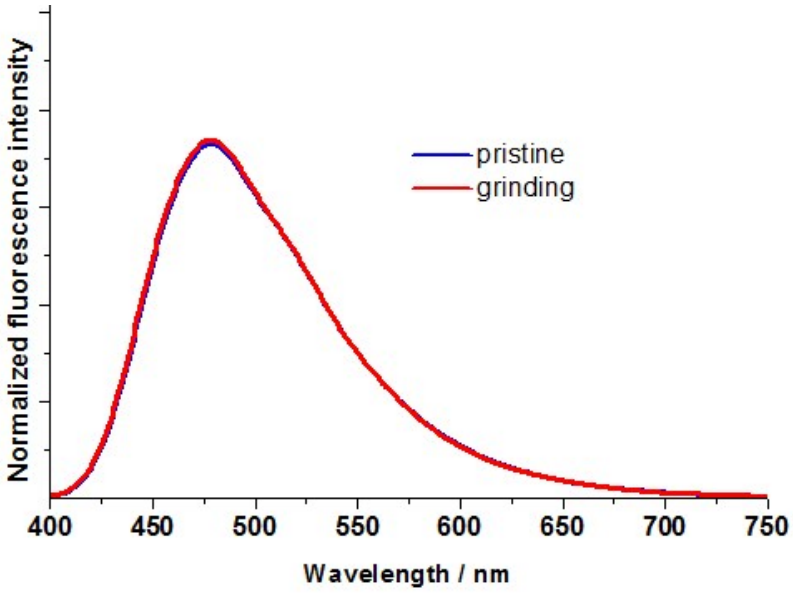

Fig. S19 Emission spectra of compound $\mathbf{V_1}$ under different solid phases

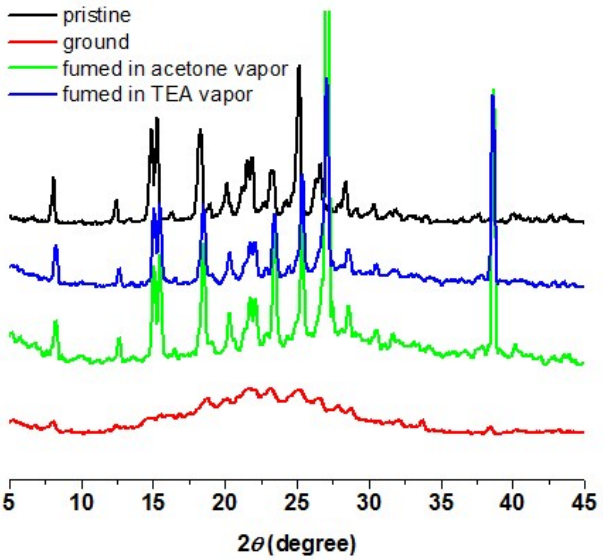

Fig. S20 PXRD patterns of compound $\mathbf{X_1}$ under different phases

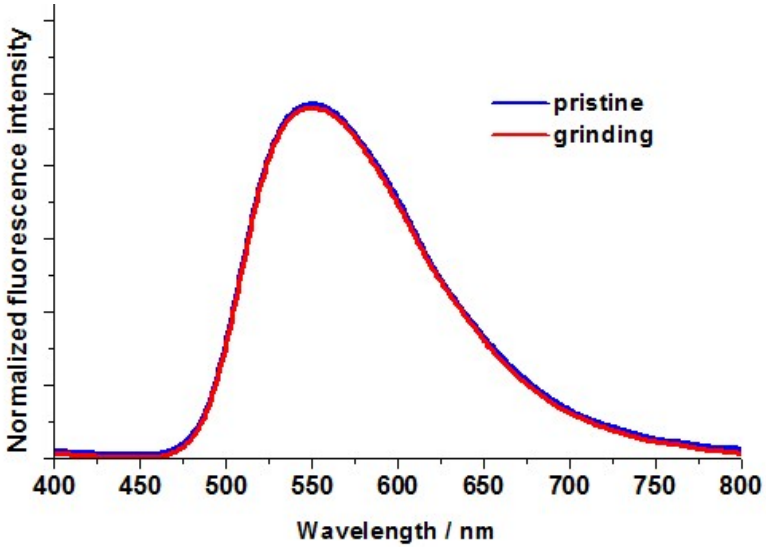

Fig. S21 Emission spectra of compound $\mathbf{X_1}$ under different solid phases

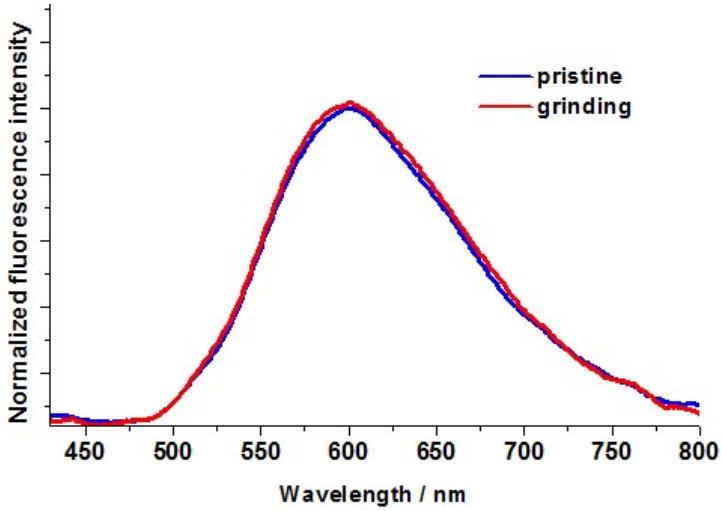

Fig. S22 Emission spectra of compound $\mathbf{X_2}$ under different solid phases

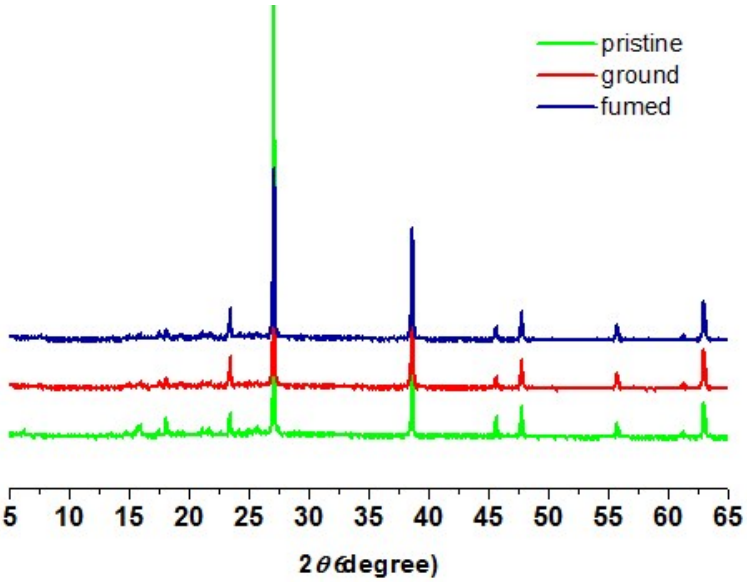

Fig. S23 PXRD patterns of compound **X**, under different phases

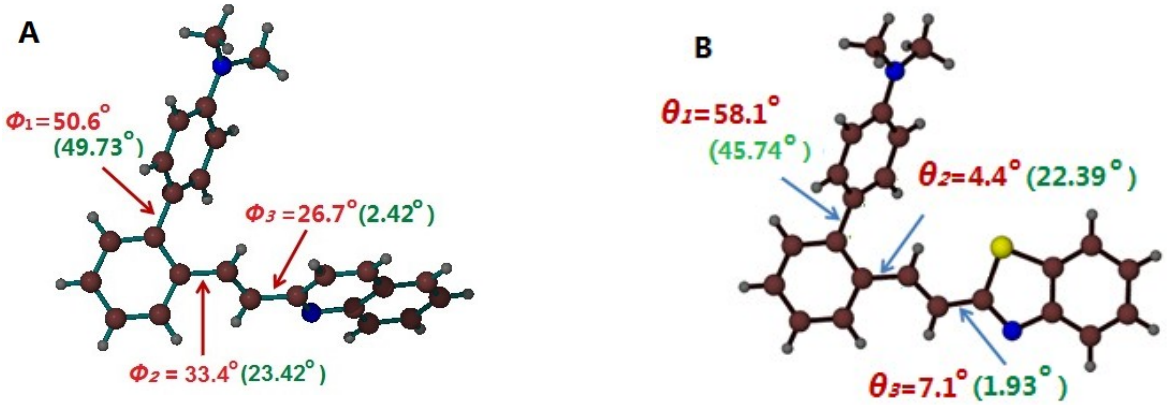

Fig. S24 Geometries of $\mathbf{V_2}$ (A) and $\mathbf{V_3}$ (B) in crystalline phase by X-ray crystallography (red) and in gas phase by Gaussian 09w calculations based on B3LYP/6-31G(d,p) basis (green)

Table S1 Emission wavelengths of $\mathbf{V_1}$-$\mathbf{V_4}$ and $\mathbf{X_1}$-$\mathbf{X_2}$ in different solvents

Compound	*n*-hexane	benzene	dichloromethane	acetone	ethanol
$\mathbf{V_1}$	410	425	434	439	446
$\mathbf{V_2}$	444	483	529	569	570
$\mathbf{V_3}$	460	513	550	568	588
$\mathbf{V_4}$	395	410	427	432	439
$\mathbf{X_1}$	442, 464	450, 473	452, 474	446, 468	455, 477
$\mathbf{X_2}$	511	525	560	585	597

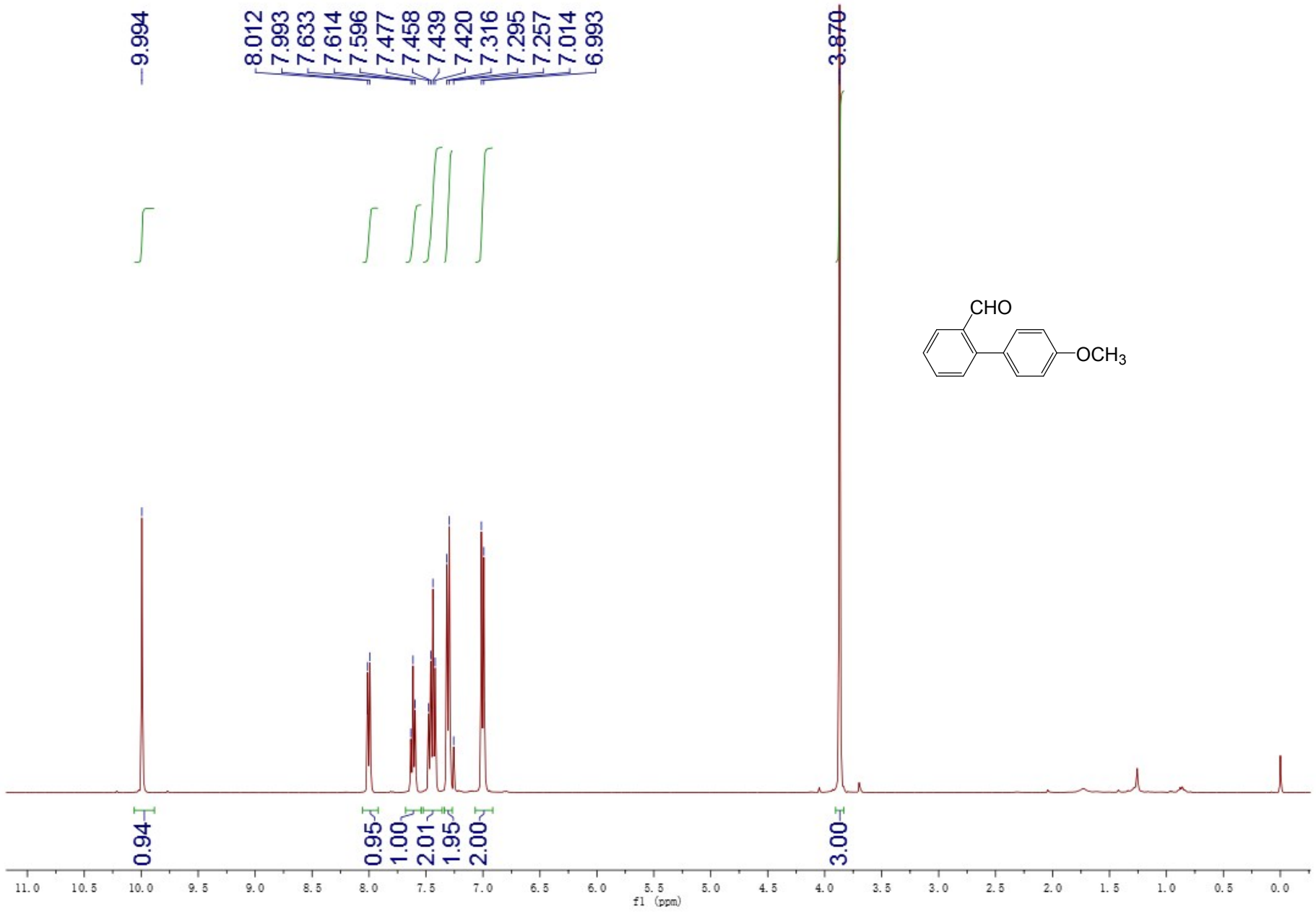
9.994
8.012
7.993
7.633
7.614
7.596
7.477
7.458
7.439
7.420
7.316
7.295
7.257
7.014
6.993
3.870
CHO
OCH3
0.94
0.95
1.00
2.01
1.95
2.00
3.00
11.0
10.5
10.0
9.5
9.0
8.5
8.0
7.5
7.0
6.5
6.0
5.5
5.0
4.5
4.0
3.5
3.0
2.5
2.0
1.5
1.0
0.5
0.0
f1 (ppm)

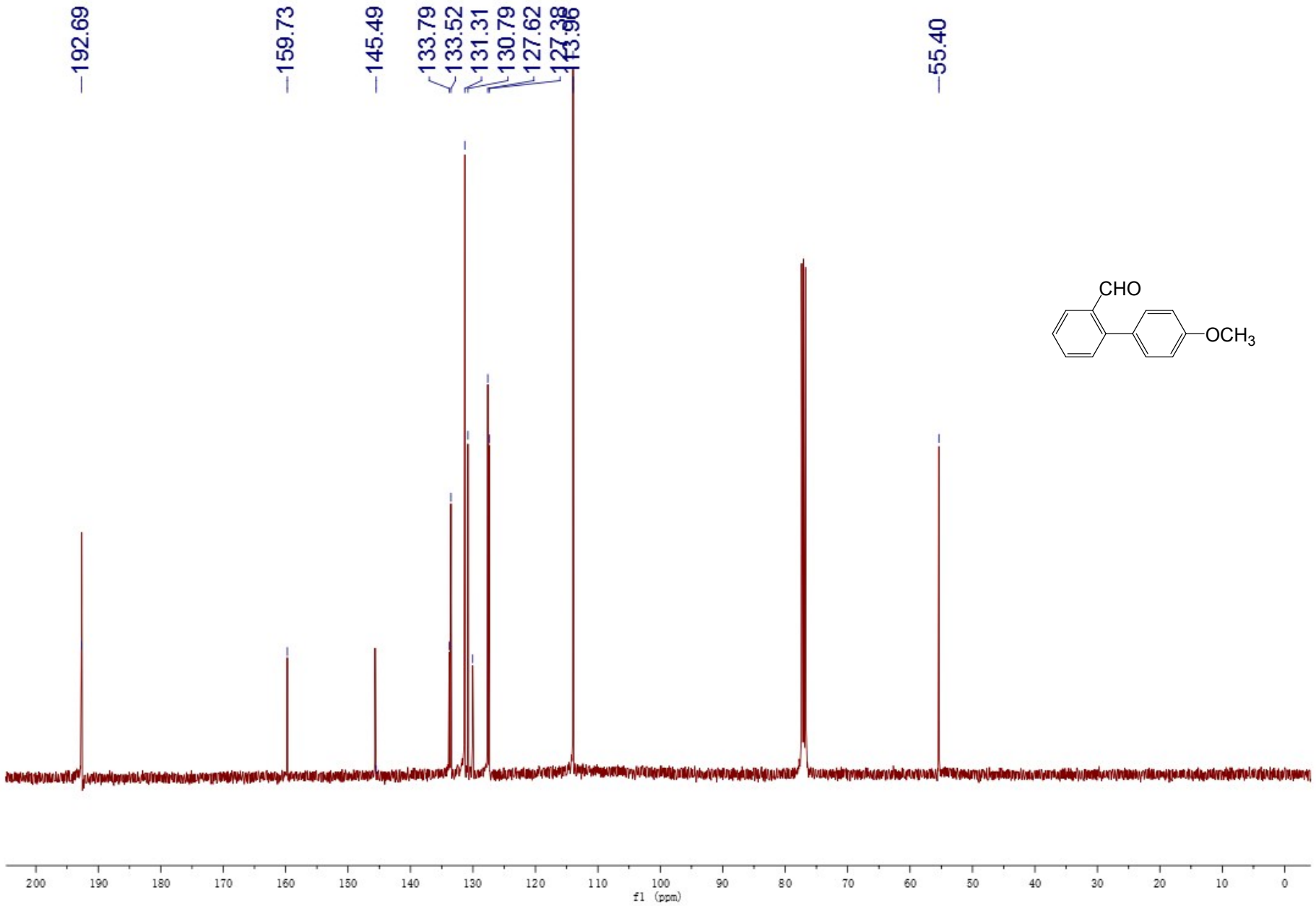
192.69
159.73
145.49
133.79
133.52
131.31
130.79
127.62
127.38
113.96
55.40
CHO
OCH3
200
190
180
170
160
150
140
130
120
110
100
90
80
70
60
50
40
30
20
10
0
f1 (ppm)

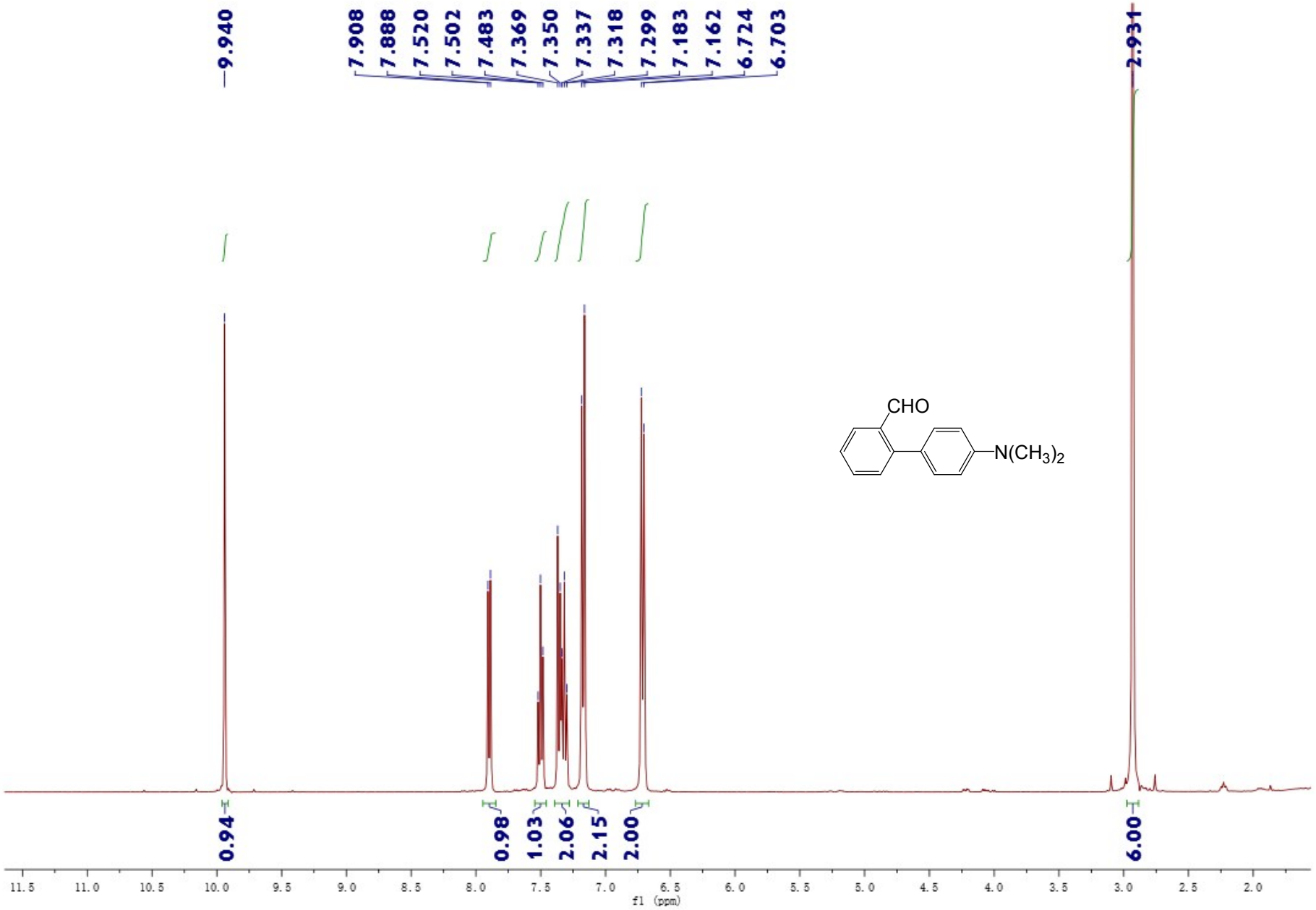
9.940
7.908
7.888
7.520
7.502
7.483
7.369
7.350
7.337
7.318
7.299
7.183
7.162
6.724
6.703
2.931
CHO
N(CH3)2
0.94
0.98
1.03
2.06
2.15
2.00
6.00
11.5
11.0
10.5
10.0
9.5
9.0
8.5
8.0
7.5
7.0
6.5
6.0
5.5
5.0
4.5
4.0
3.5
3.0
2.5
2.0
f1 (ppm)

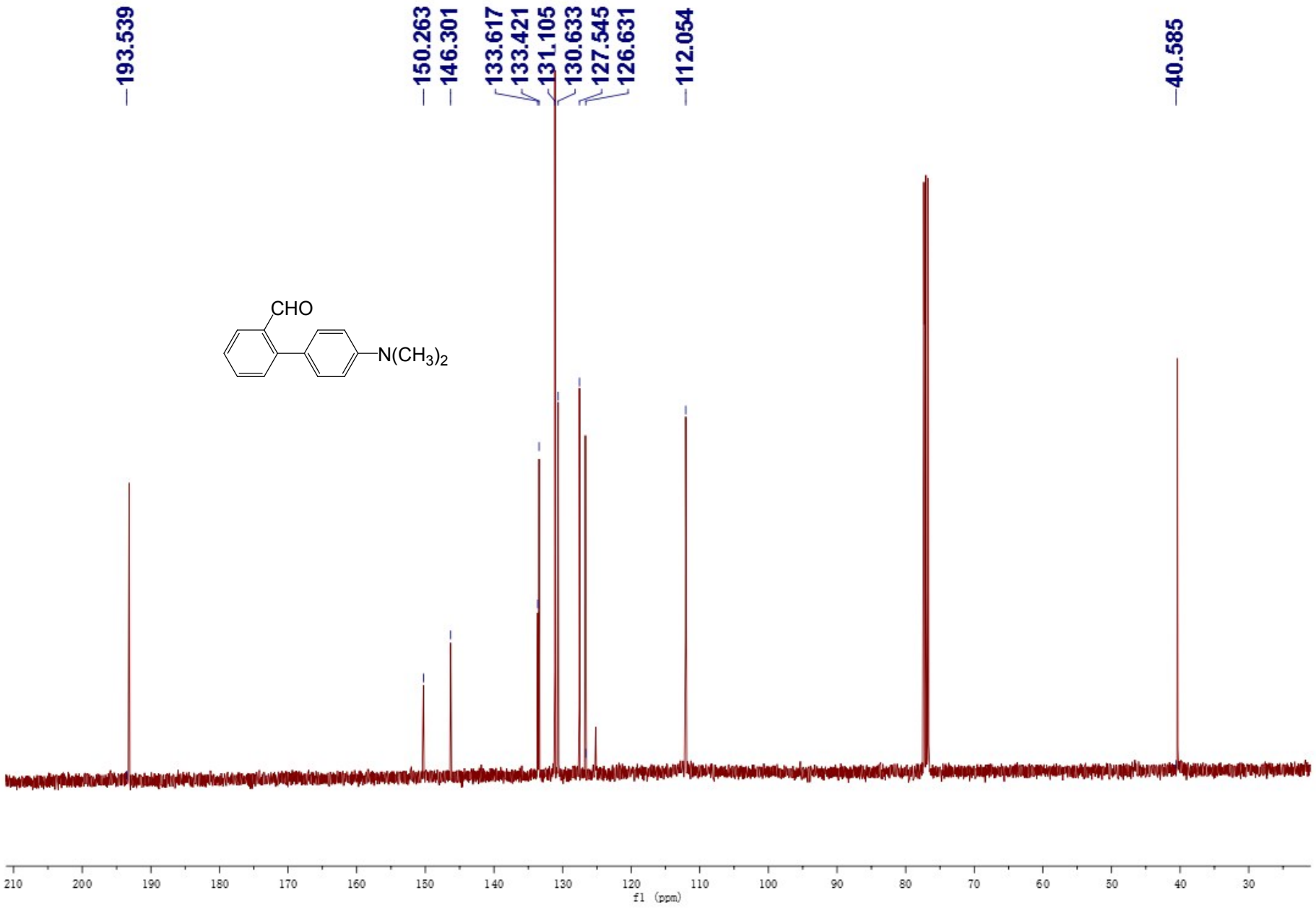
193.539
150.263
146.301
133.617
133.421
131.105
130.633
127.545
126.631
112.054
40.585
CHO
N(CH3)2
210
200
190
180
170
160
150
140
130
120
110
100
90
80
70
60
50
40
30
f1 (ppm)

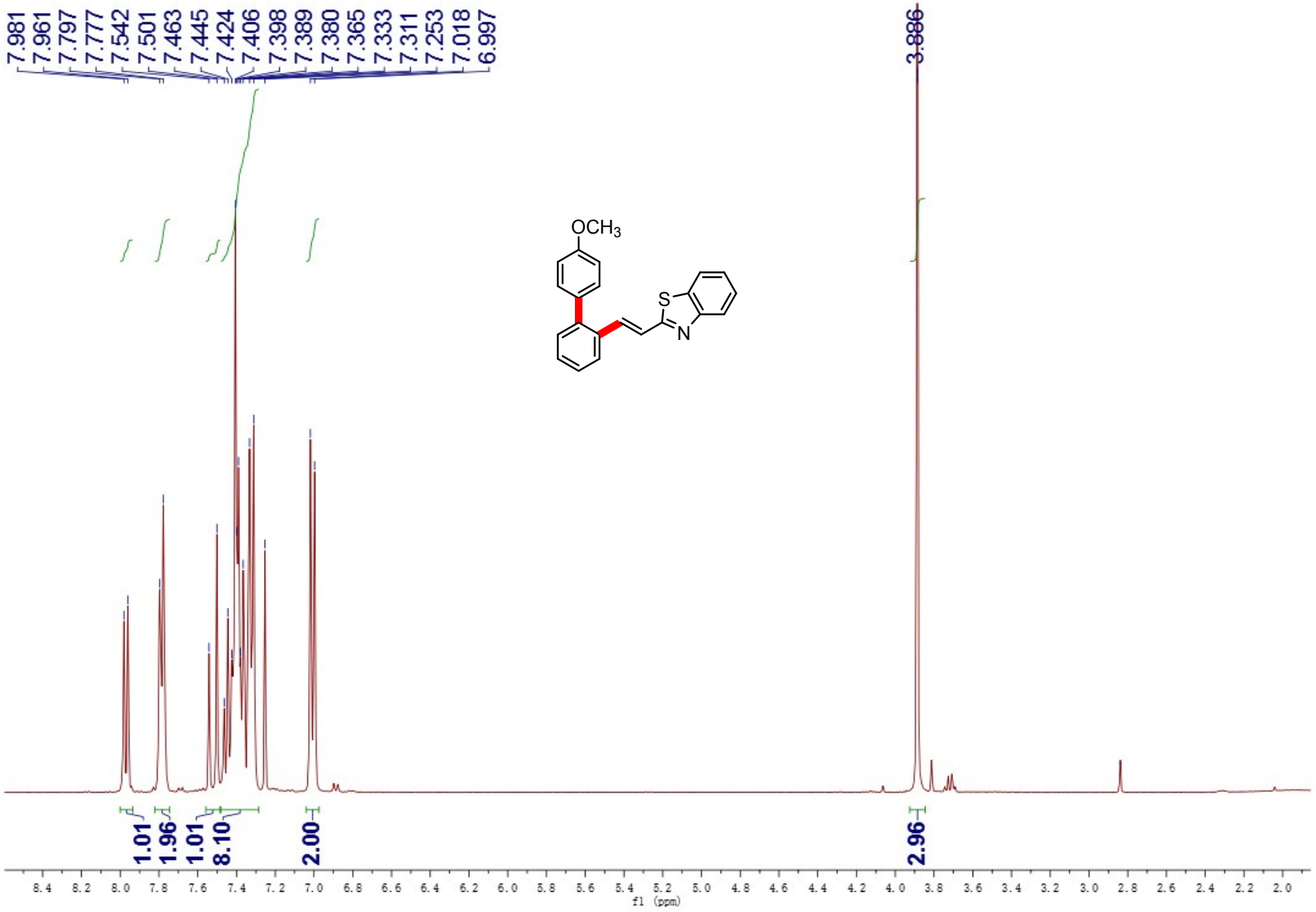
7.981
7.961
7.797
7.777
7.542
7.501
7.463
7.445
7.424
7.406
7.398
7.389
7.380
7.365
7.333
7.311
7.253
7.018
6.997
3.886
OCH3
S
N
1.01
1.96
1.01
8.10
2.00
2.96
f1 (ppm)

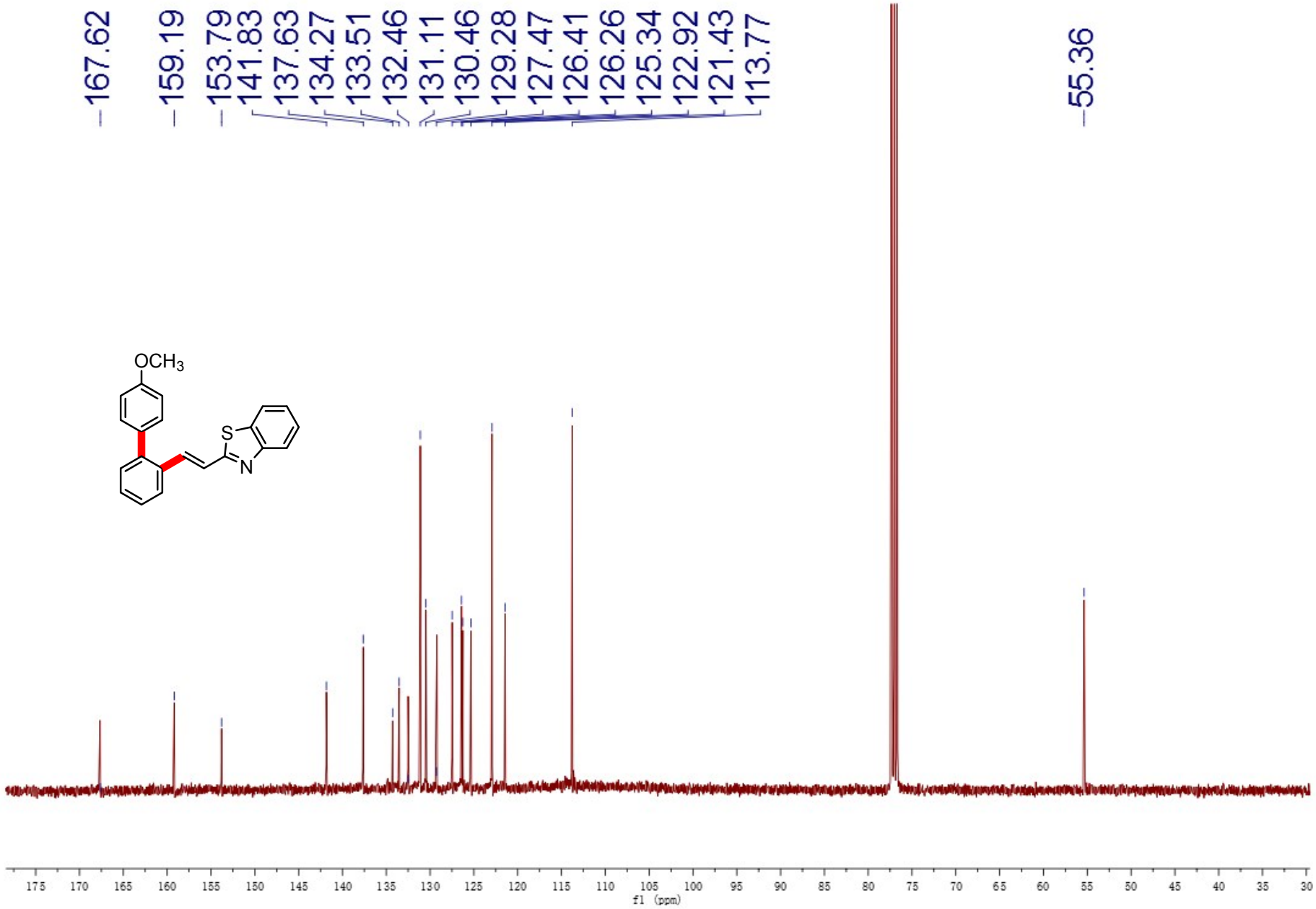
167.62
159.19
153.79
141.83
137.63
134.27
133.51
132.46
131.11
130.46
129.28
127.47
126.41
126.26
125.34
122.92
121.43
113.77
55.36
OCH3
S
N
175 170 165 160 155 150 145 140 135 130 125 120 115 110 105 100 95 90 85 80 75 70 65 60 55 50 45 40 35 30
f1 (ppm)

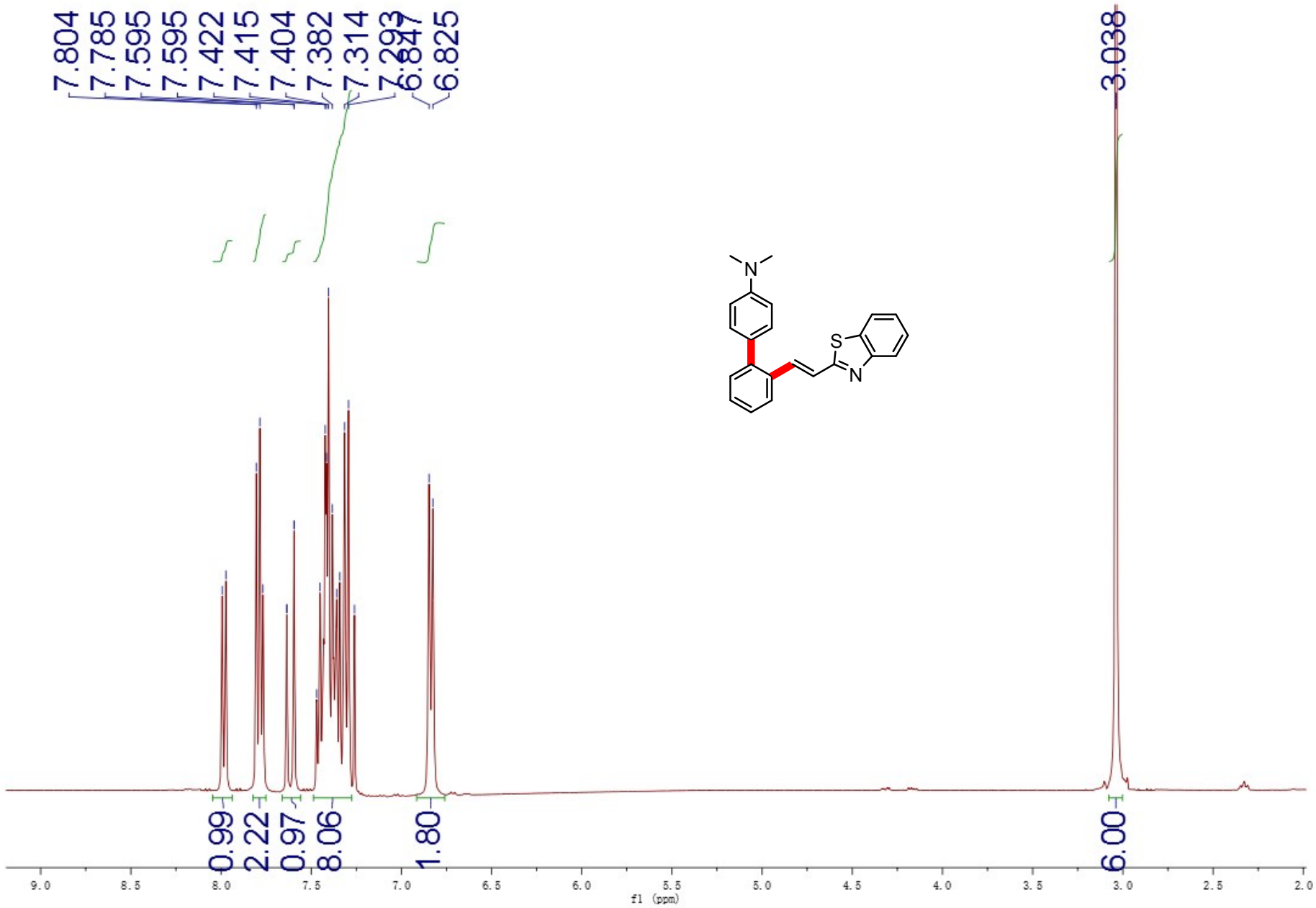
7.804
7.785
7.595
7.595
7.422
7.415
7.404
7.382
7.314
7.293
6.847
6.825
3.038
N
S
N
0.99
2.22
0.97
8.06
1.80
6.00
9.0
8.5
8.0
7.5
7.0
6.5
6.0
5.5
5.0
4.5
4.0
3.5
3.0
2.5
2.0
f1 (ppm)

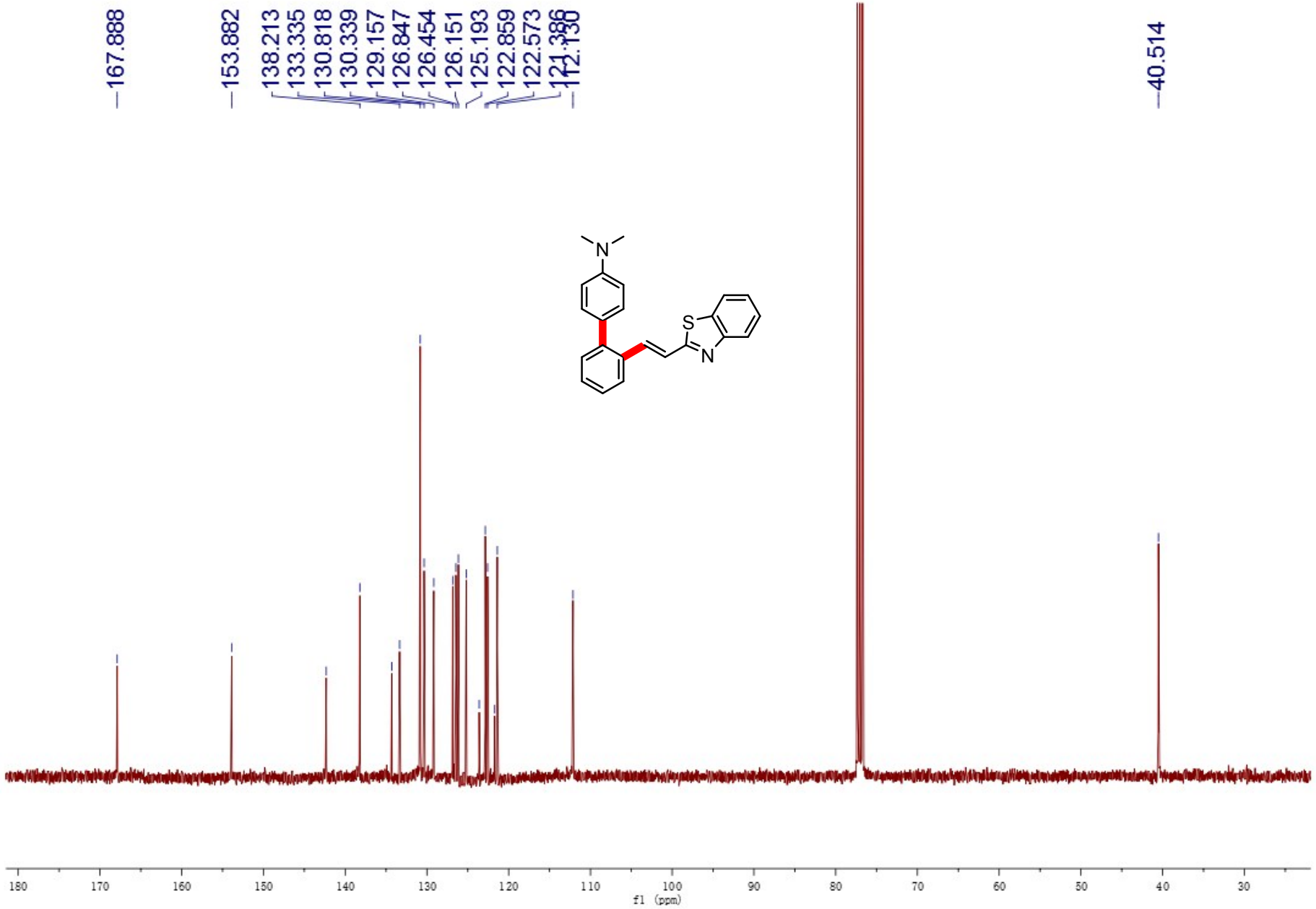
167.888
153.882
138.213
133.335
130.818
130.339
129.157
126.847
126.454
126.151
125.193
122.859
122.573
121.386
112.130
40.514
N
S
N
180
170
160
150
140
130
120
110
100
90
80
70
60
50
40
30
f1 (ppm)

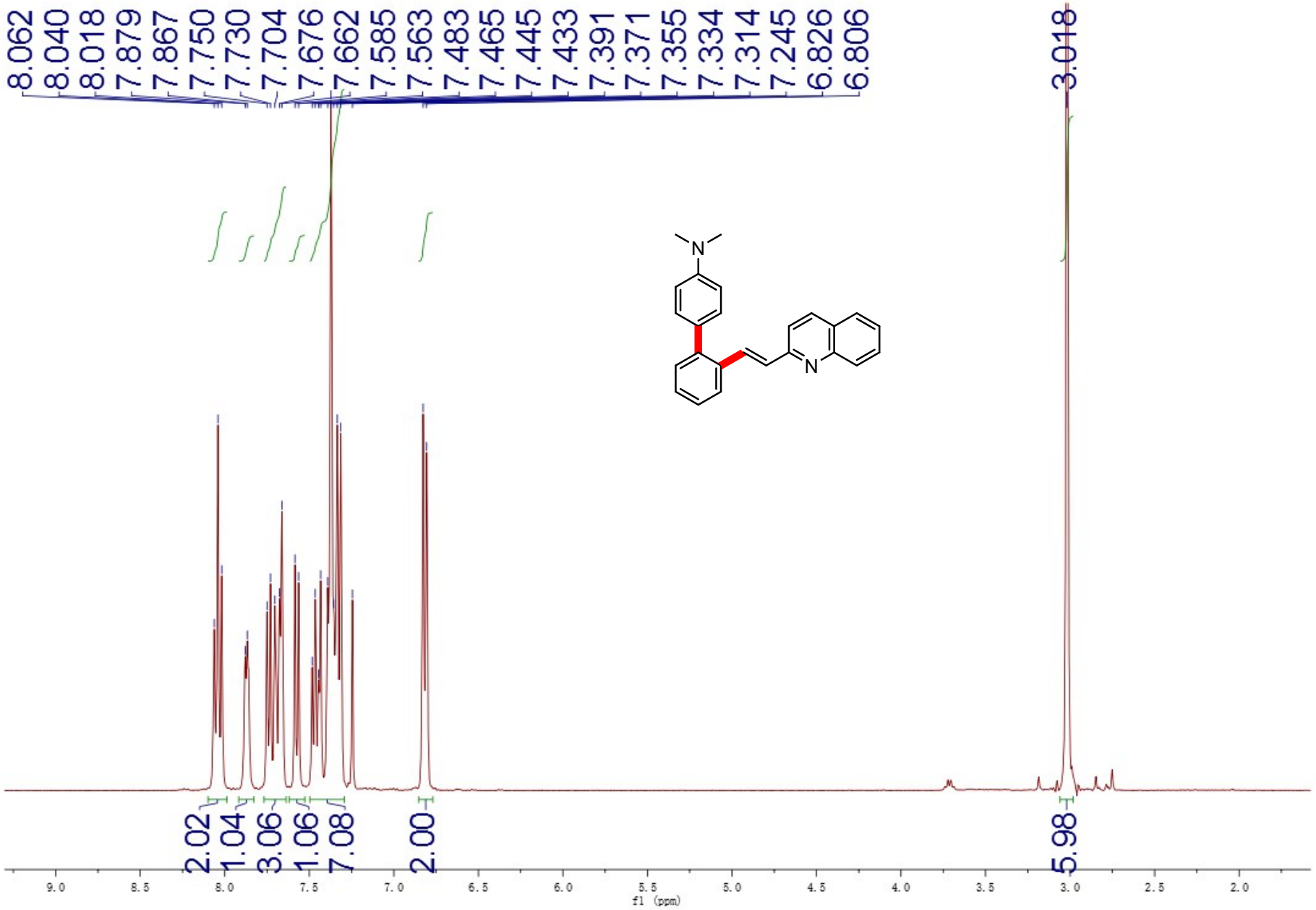
8.062
8.040
8.018
7.879
7.867
7.750
7.730
7.704
7.676
7.662
7.585
7.563
7.483
7.465
7.445
7.433
7.391
7.371
7.355
7.334
7.314
7.245
6.826
6.806
3.018
N
N
2.02
1.04
3.06
1.06
7.08
2.00
5.98
9.0
8.5
8.0
7.5
7.0
6.5
6.0
5.5
5.0
4.5
4.0
3.5
3.0
2.5
2.0
f1 (ppm)

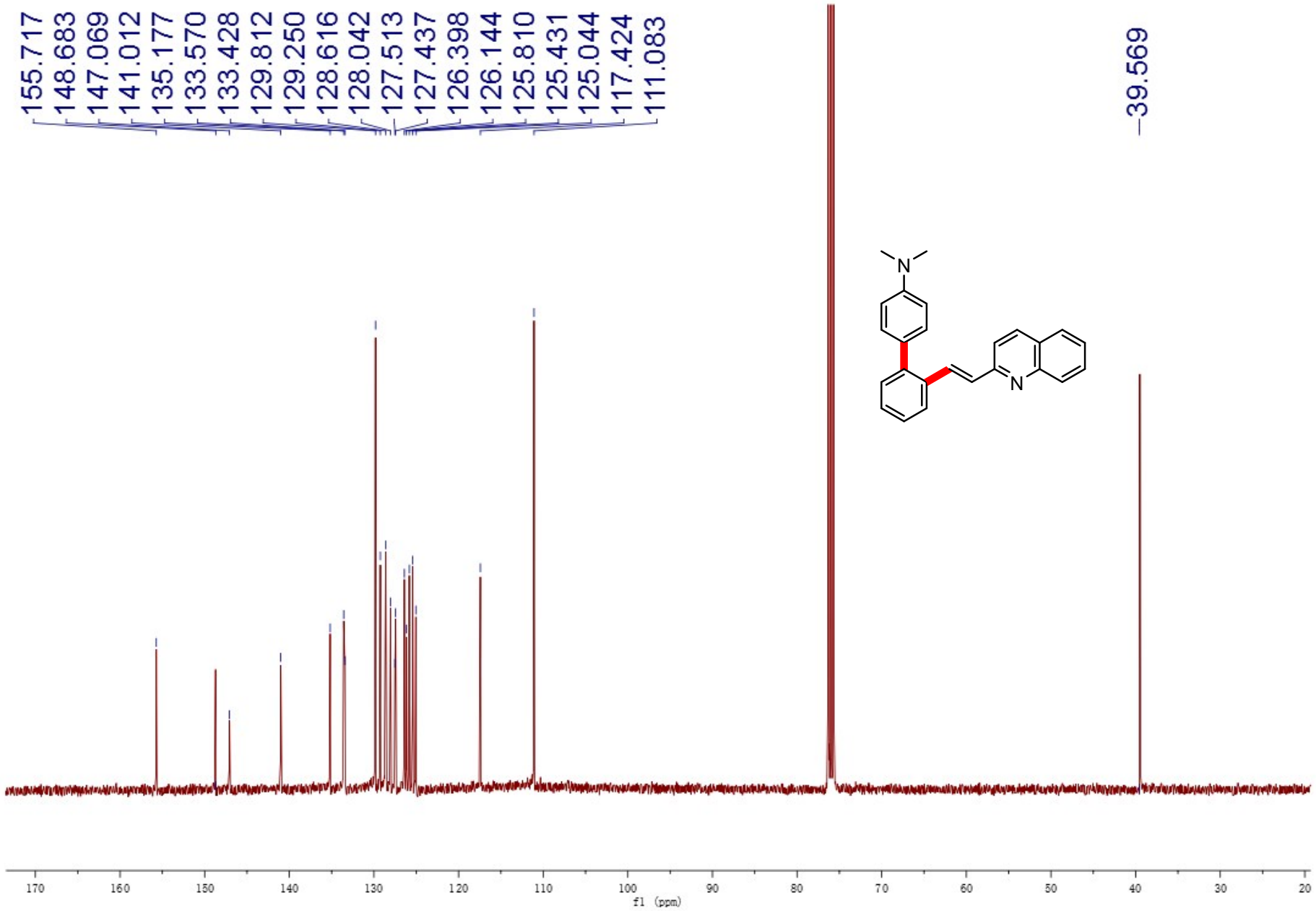
155.717
148.683
147.069
141.012
135.177
133.570
133.428
129.812
129.250
128.616
128.042
127.513
127.437
126.398
126.144
125.810
125.431
125.044
117.424
111.083
39.569
N
N
170
160
150
140
130
120
110
100
90
80
70
60
50
40
30
20
f1 (ppm)

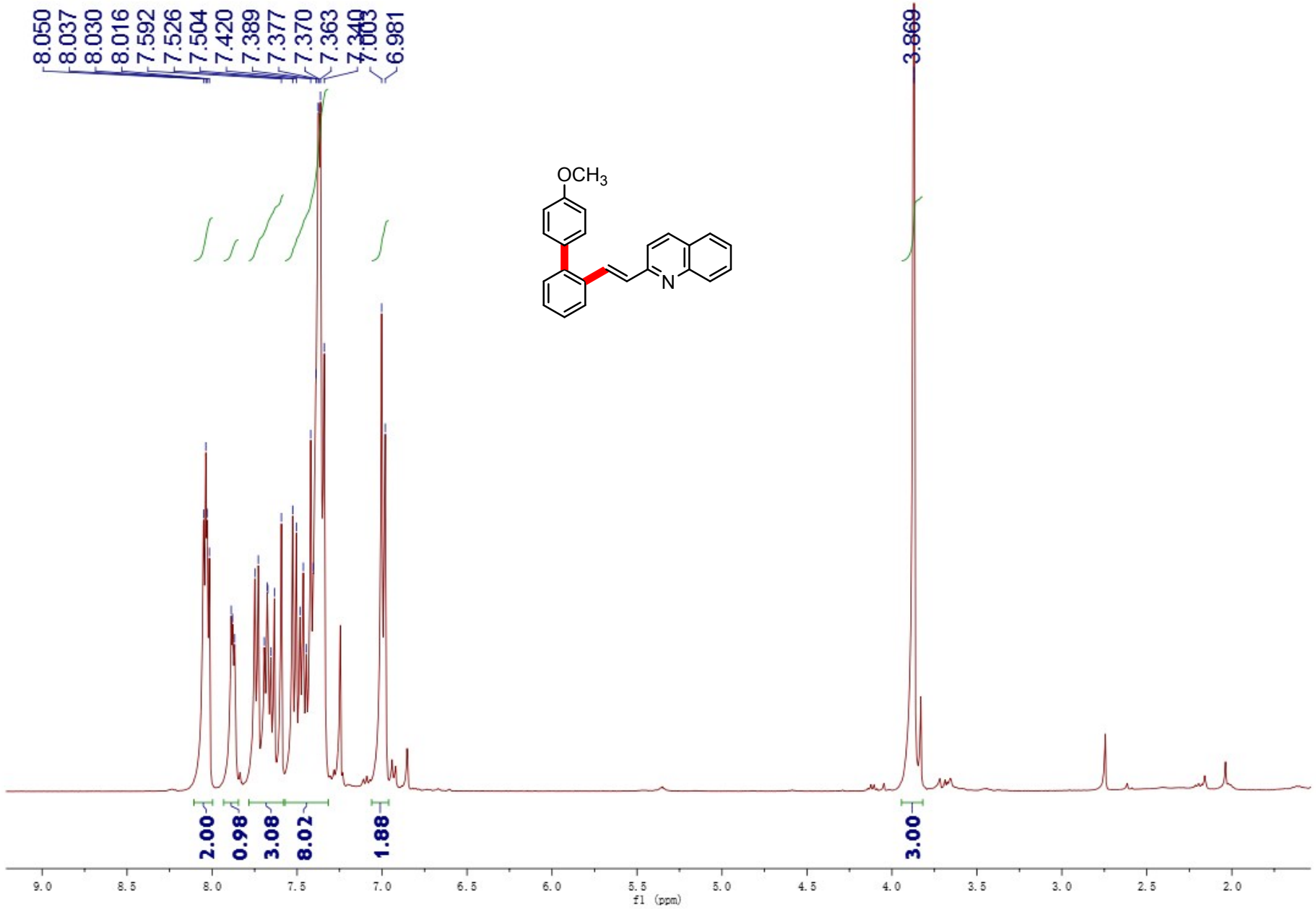
8.050
8.037
8.030
8.016
7.592
7.526
7.504
7.420
7.389
7.377
7.370
7.363
7.340
7.003
6.981
3.869
OCH3
N
2.00
0.98
3.08
8.02
1.88
3.00
9.0
8.5
8.0
7.5
7.0
6.5
6.0
5.5
5.0
4.5
4.0
3.5
3.0
2.5
2.0
f1 (ppm)

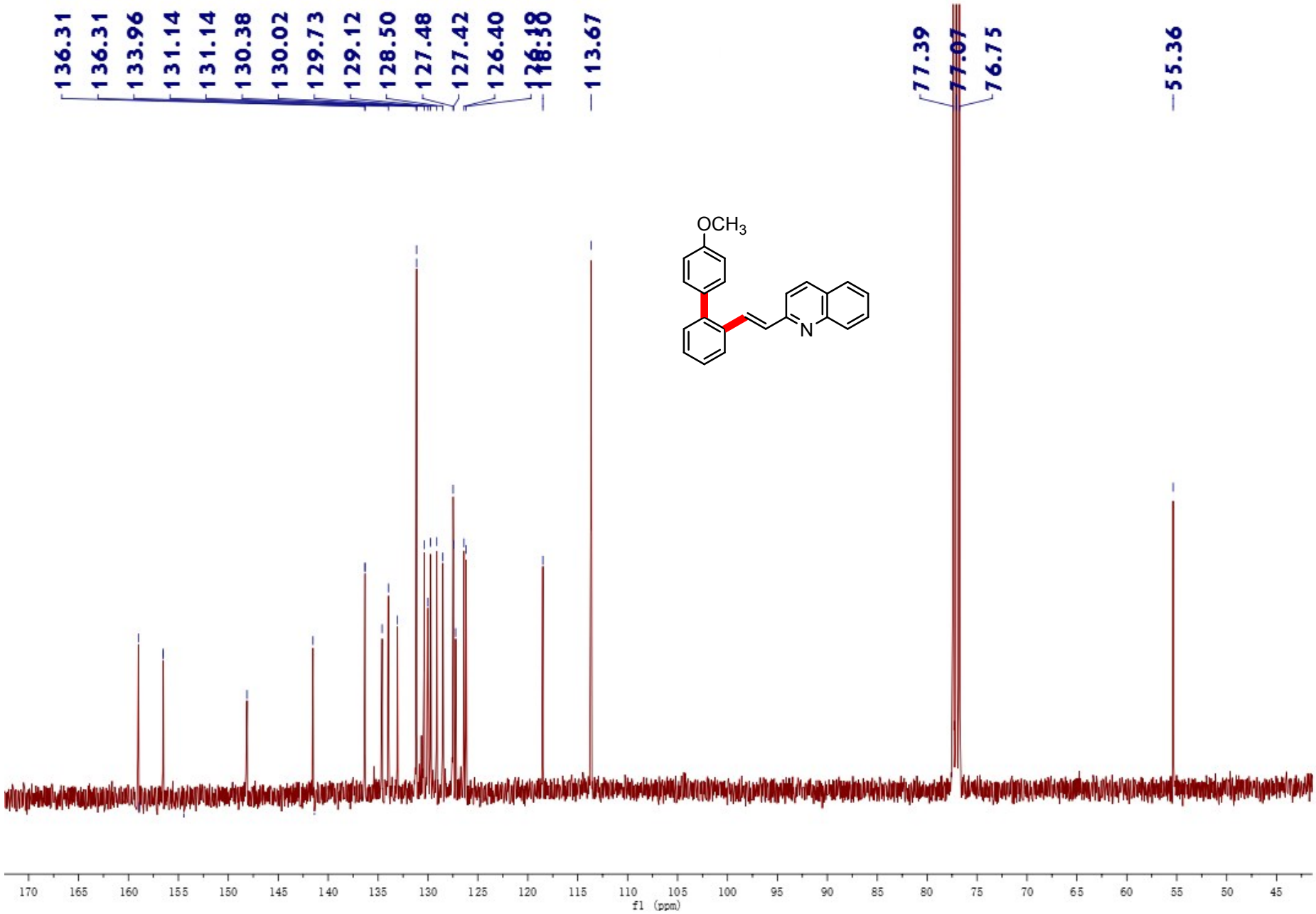
136.31
136.31
133.96
131.14
131.14
130.38
130.02
129.73
129.12
128.50
127.48
127.42
126.40
113.67
77.39
77.07
76.75
55.36
OCH3
N
170 165 160 155 150 145 140 135 130 125 120 115 110 105 100 95 90 85 80 75 70 65 60 55 50 45
f1 (ppm)

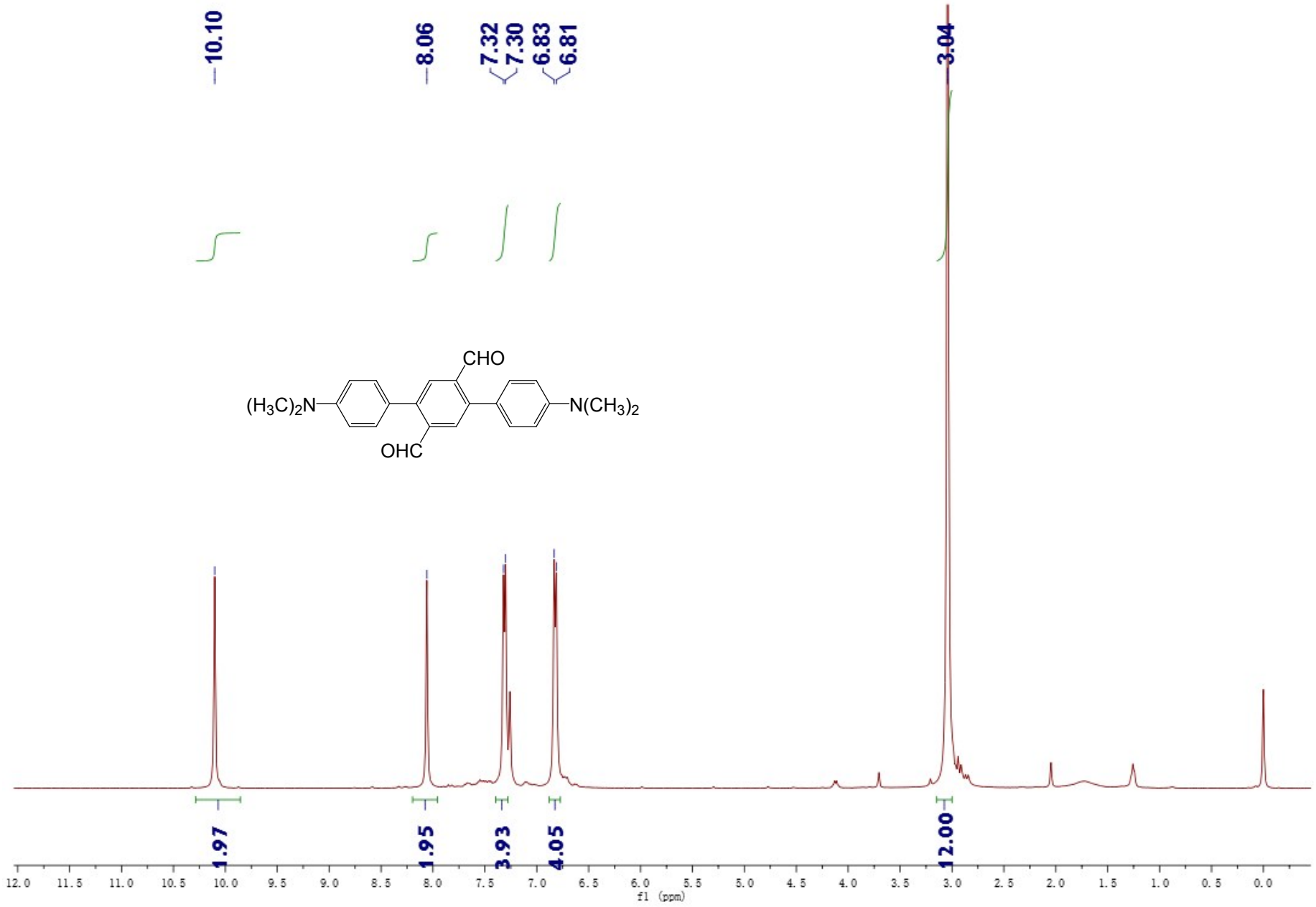
10.10
8.06
7.32
7.30
6.83
6.81
3.04
CHO
(H3C)2N
N(CH3)2
OHC
1.97
1.95
3.93
4.05
12.00
f1 (ppm)

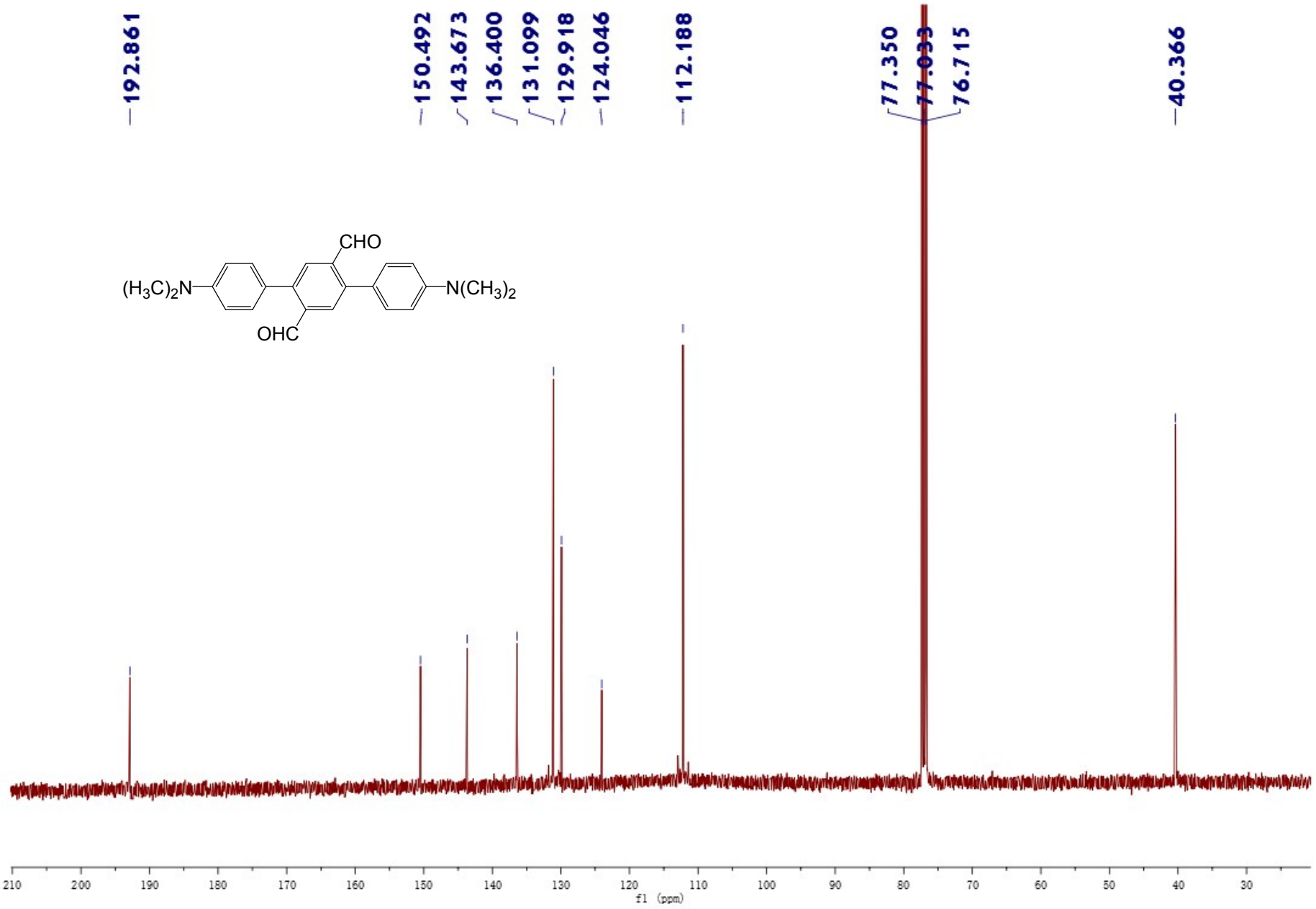
192.861
150.492
143.673
136.400
131.099
129.918
124.046
112.188
77.350
77.033
76.715
40.366
CHO
(H3C)2N
N(CH3)2
OHC
210
200
190
180
170
160
150
140
130
120
110
100
90
80
70
60
50
40
30
f1 (ppm)

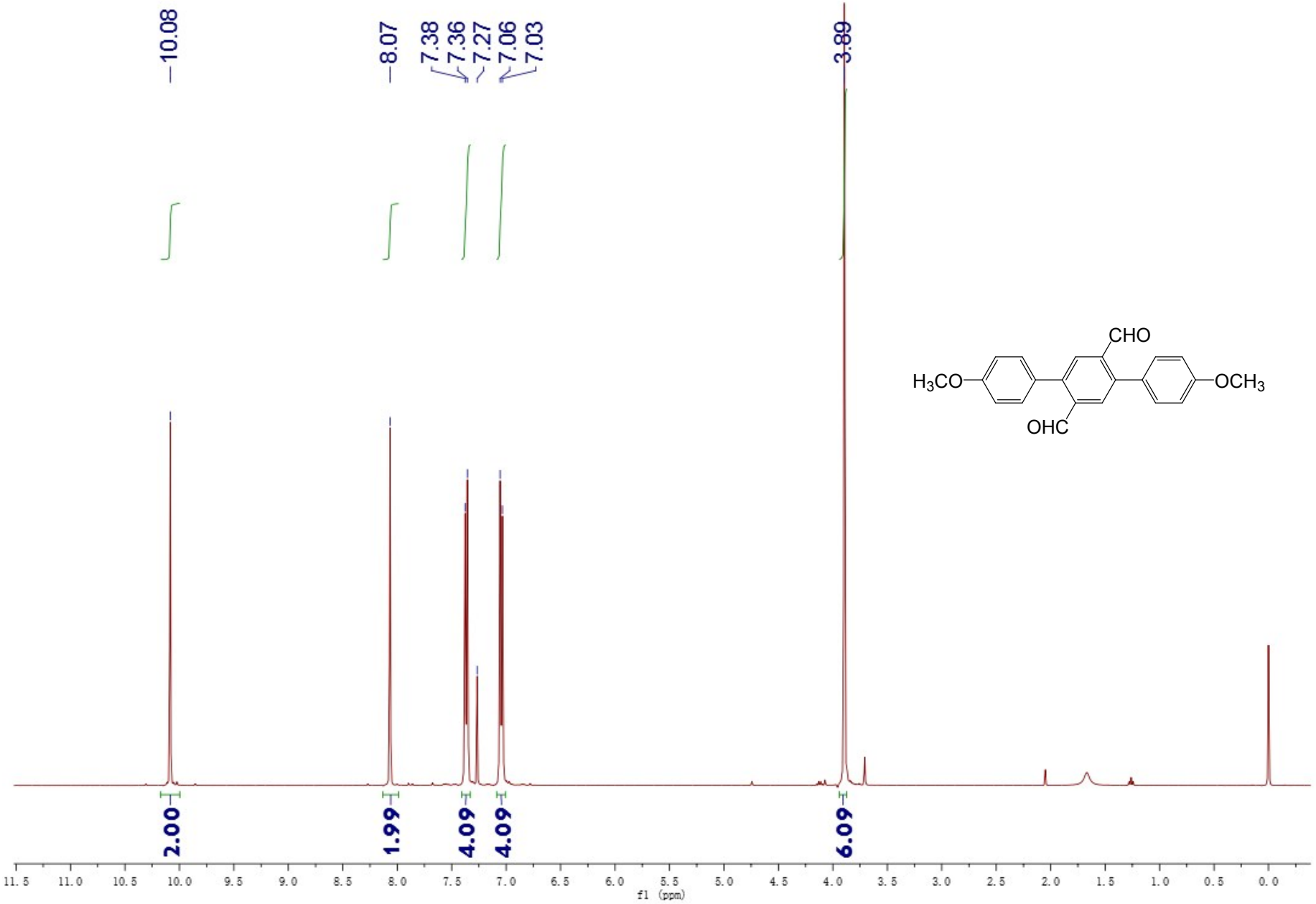
10.08
8.07
7.38
7.36
7.27
7.06
7.03
3.89
CHO
H3CO
OCH3
OHC
2.00
1.99
4.09
4.09
6.09
f1 (ppm)

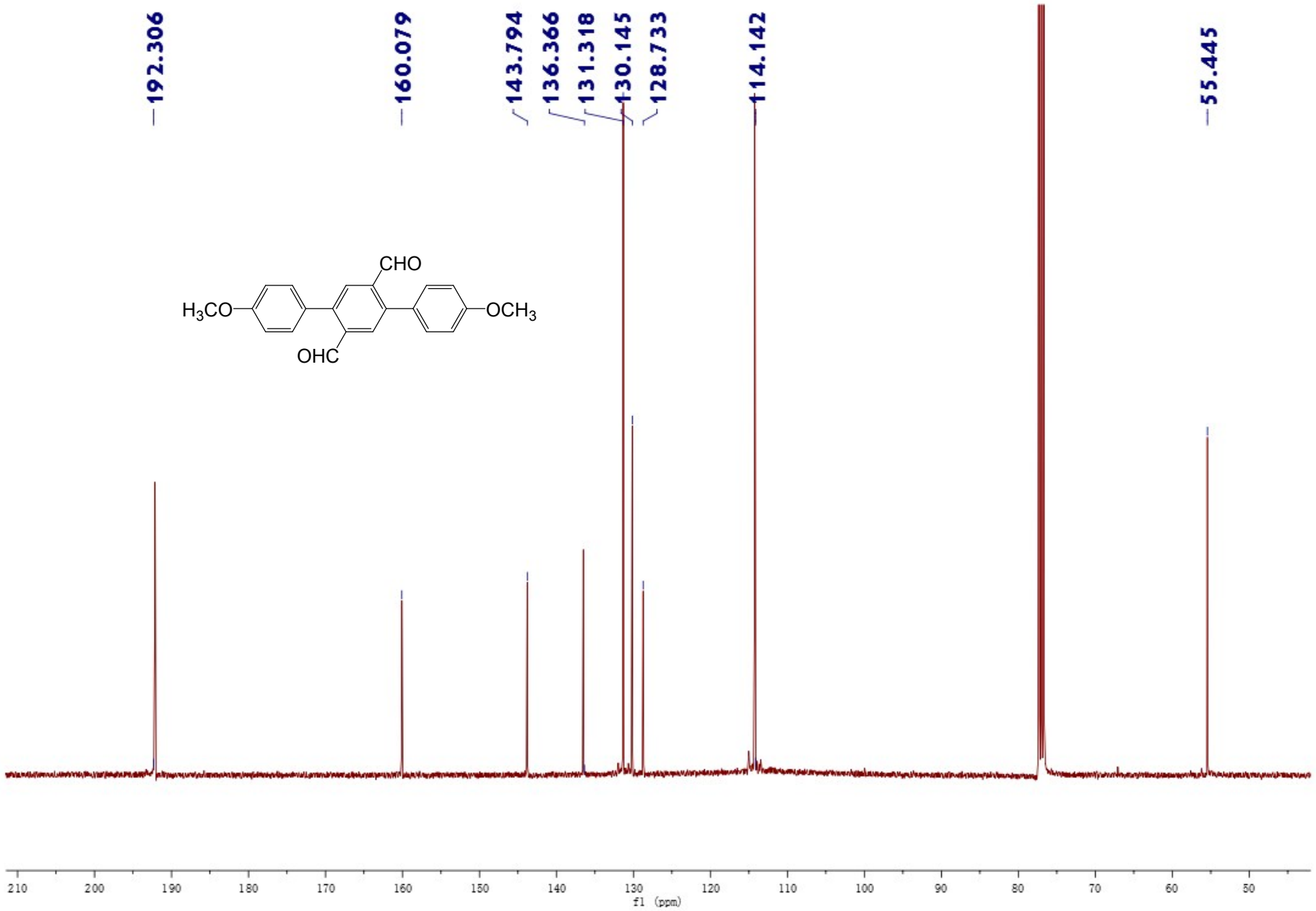
192.306
160.079
143.794
136.366
131.318
130.145
128.733
114.142
55.445
CHO
H3CO
OCH3
OHC
210
200
190
180
170
160
150
140
130
120
110
100
90
80
70
60
50
f1 (ppm)

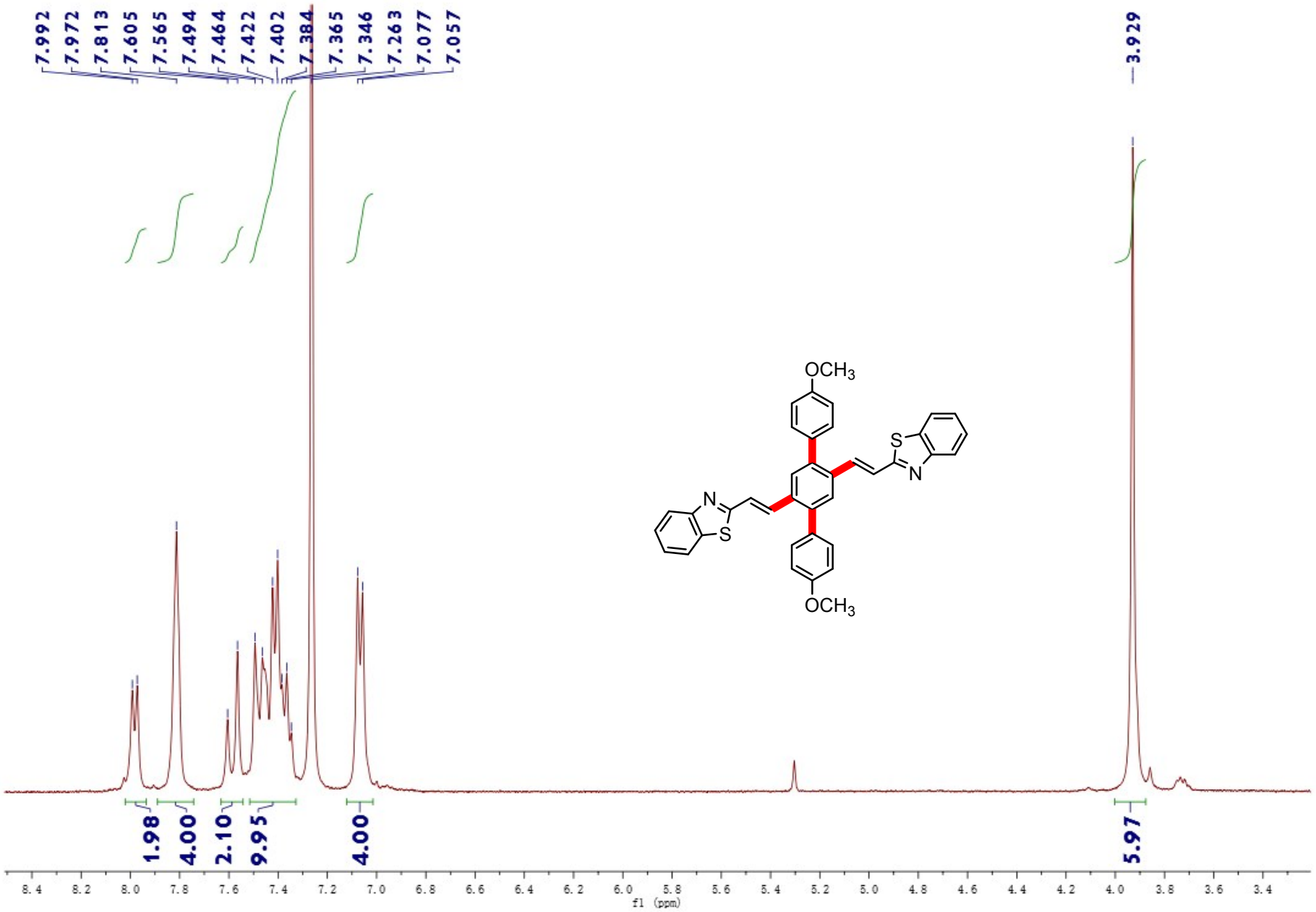
7.992
7.972
7.813
7.605
7.565
7.494
7.464
7.422
7.402
7.384
7.365
7.346
7.263
7.077
7.057
3.929
OCH3
OCH3
N
S
S
N
1.98
4.00
2.10
9.95
4.00
5.97
f1 (ppm)

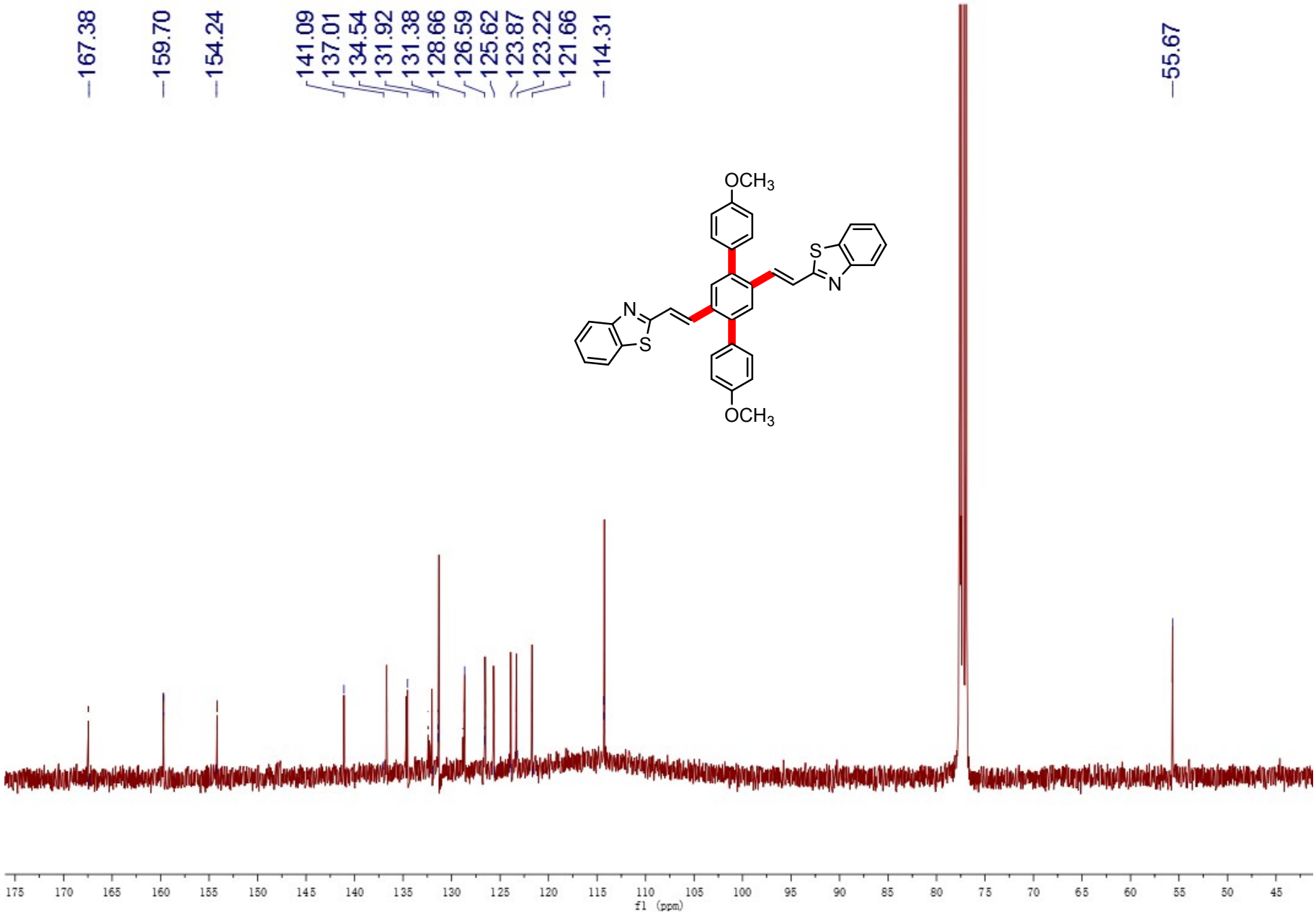
167.38
159.70
154.24
141.09
137.01
134.54
131.92
131.38
128.66
126.59
125.62
123.87
123.22
121.66
114.31
55.67
OCH3
OCH3
N
S
S
N
175 170 165 160 155 150 145 140 135 130 125 120 115 110 105 100 95 90 85 80 75 70 65 60 55 50 45
f1 (ppm)

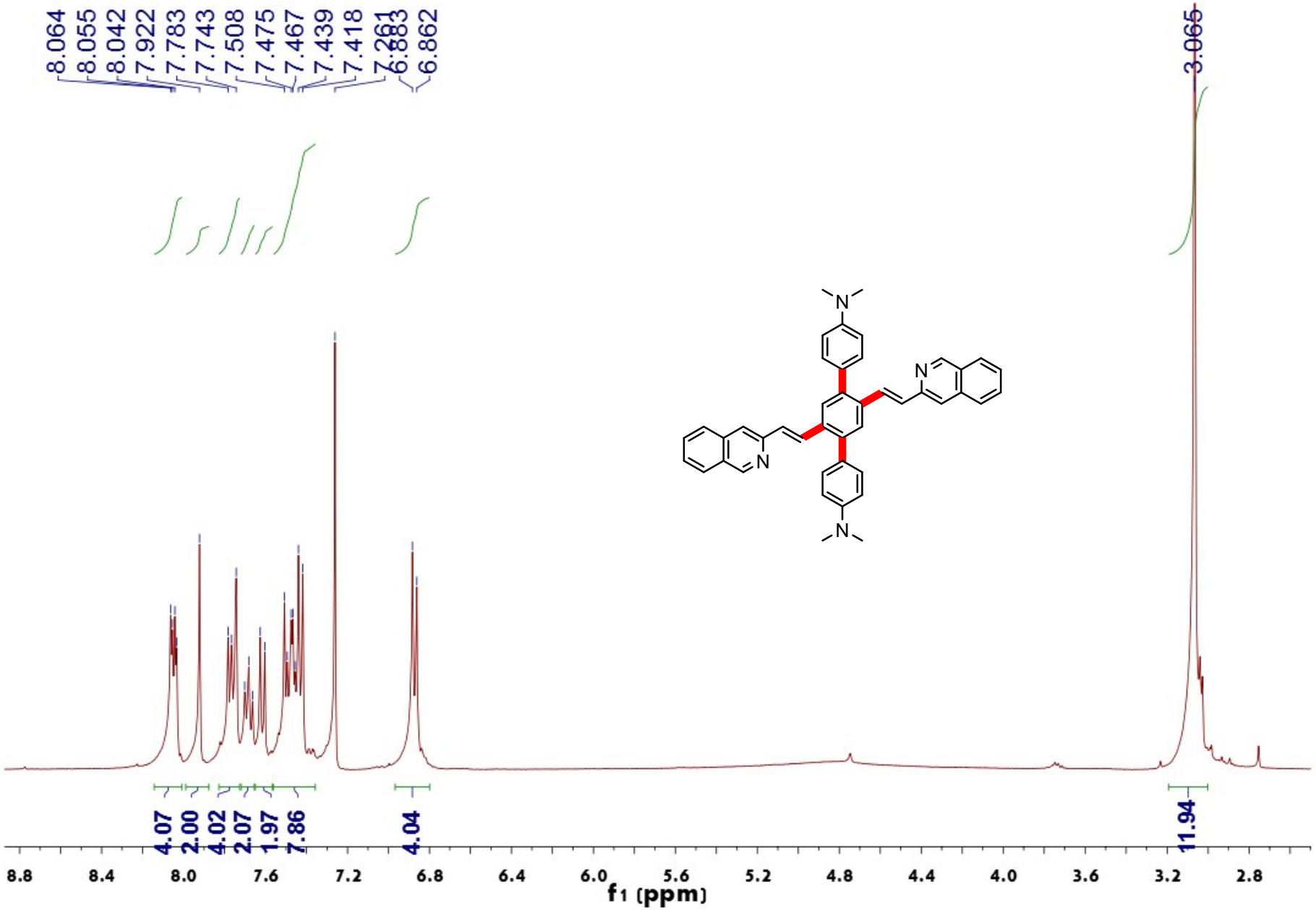
8.064
8.055
8.042
7.922
7.783
7.743
7.508
7.475
7.467
7.439
7.418
7.261
6.883
6.862
3.065
4.07
2.00
4.02
2.07
1.97
7.86
4.04
11.94
8.8
8.4
8.0
7.6
7.2
6.8
6.4
6.0
5.6
5.2
4.8
4.4
4.0
3.6
3.2
2.8
f1 (ppm)
N
N
N
N

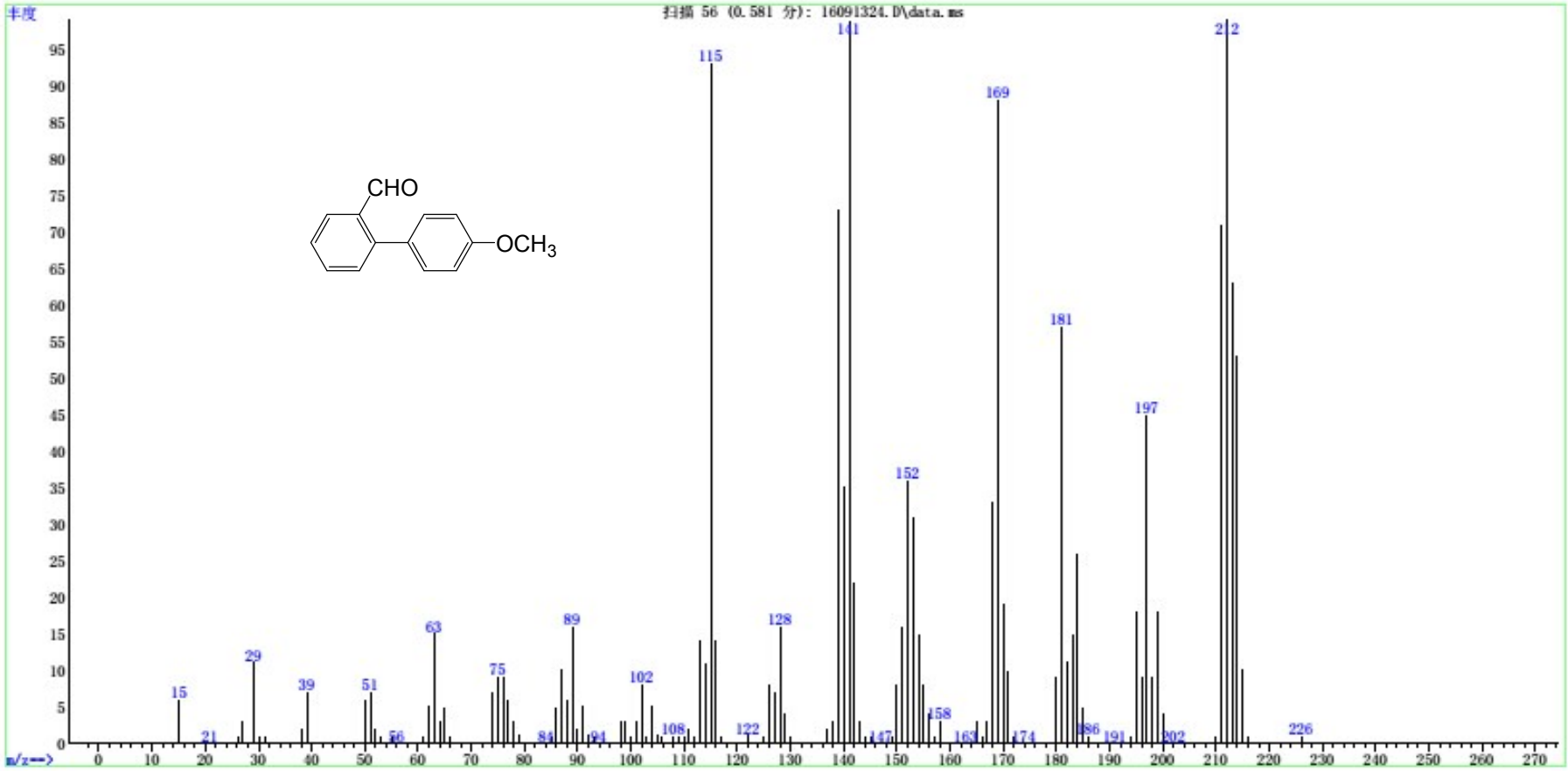
半度
扫描 56 (0.581 分): 16091324.D\data.ms
CHO
OCH3
m/z-->
115
141
212
169
181
197
152
89
128
63
75
102
29
39
51
15
21
56
84
94
108
122
147
163
174
186
191
202
226

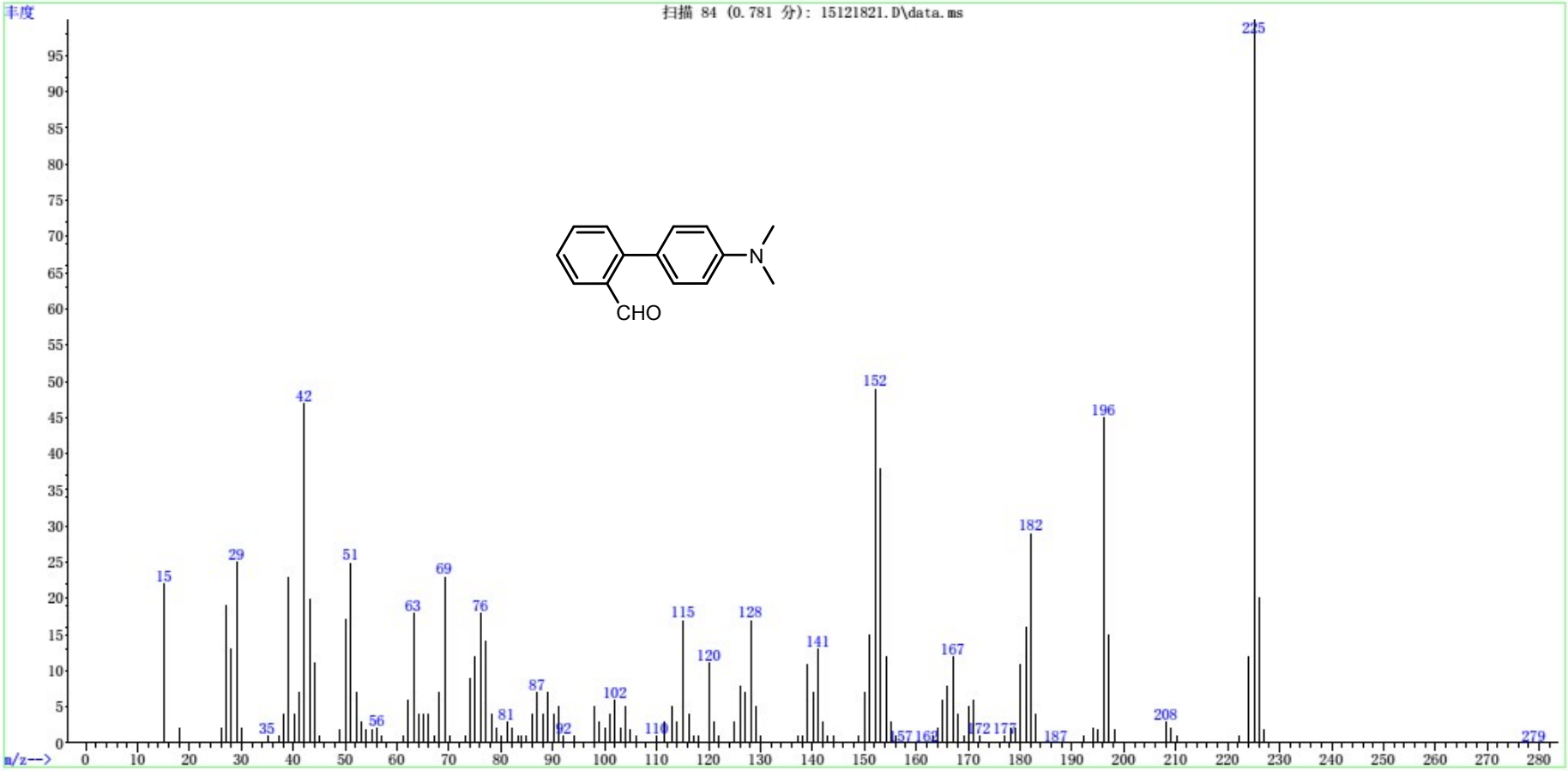
丰度
扫描 84 (0.781 分): 15121821.D\data.ms
m/z-->
CHO
N
225
152
196
182
42
69
51
29
15
63
76
115
128
141
120
167
87
102
208
279
35
56
81
92
110
157
165
172
177
187

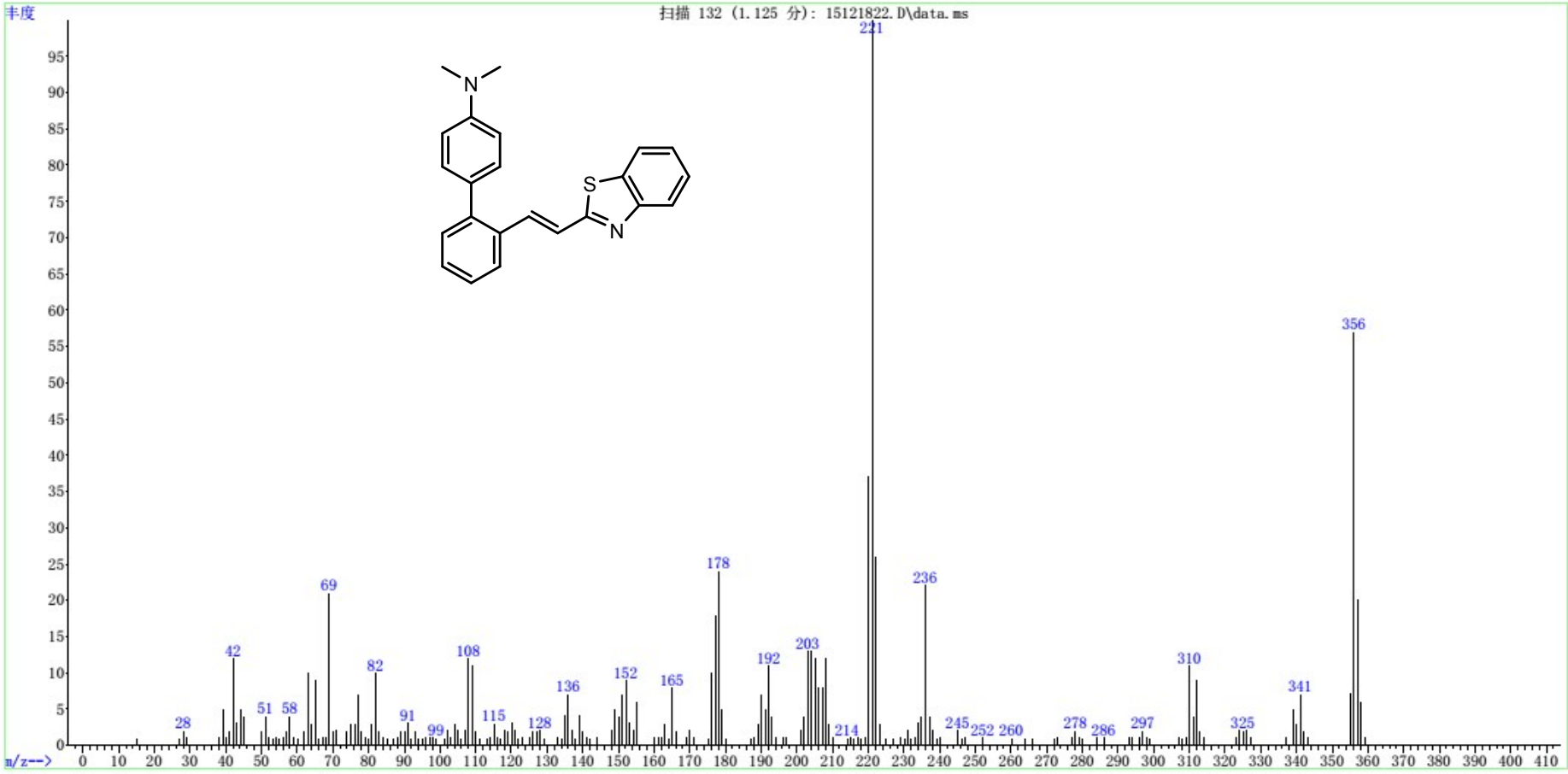
丰度
扫描 132 (1.125 分): 15121822.D\data.ms
m/z-->
N
S
N
221
356
178
69
236
42
108
82
192
203
152
136
165
310
341
91
115
128
214
245
252
260
278
286
297
325
28
51
58
99

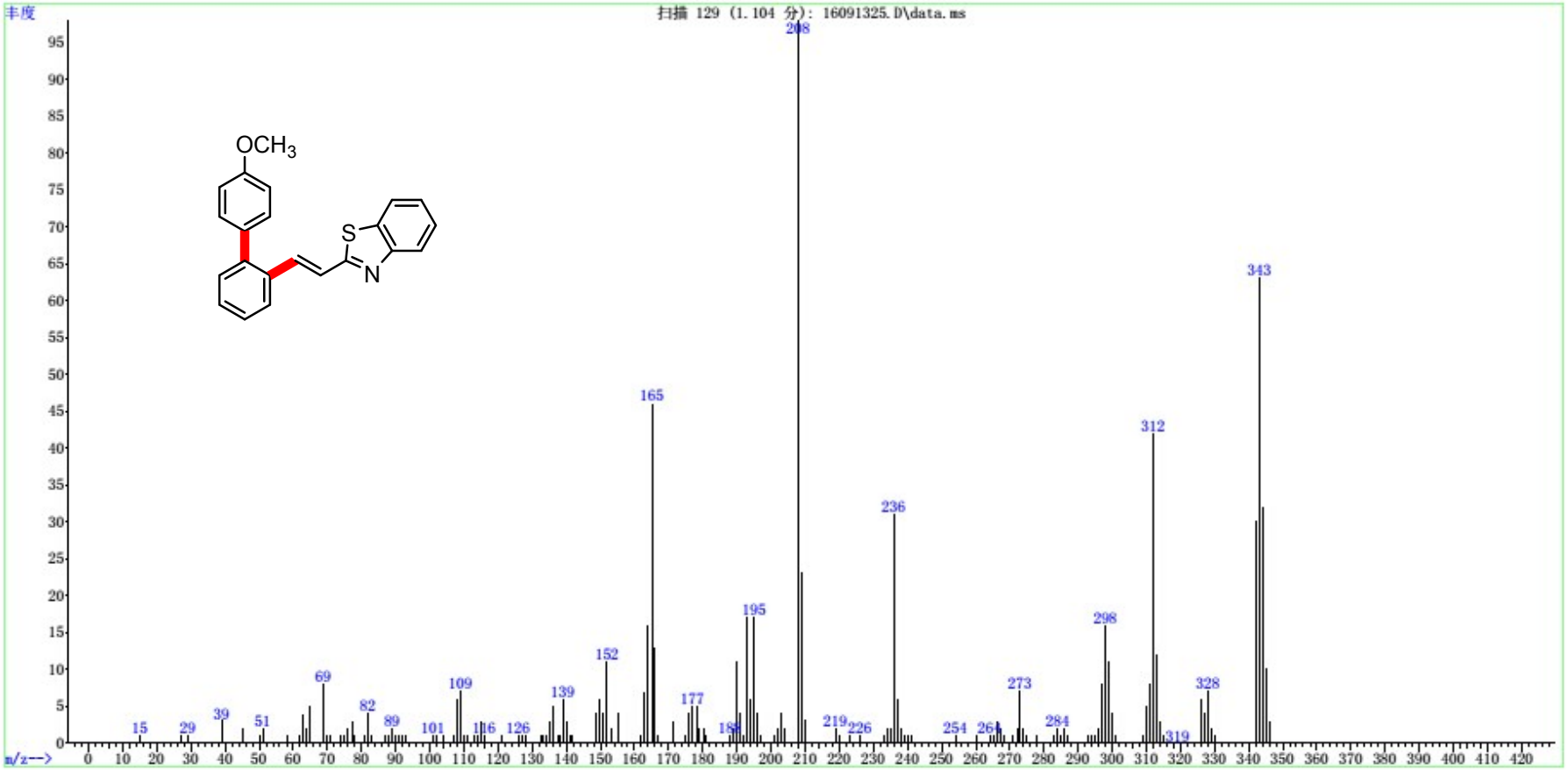
丰度
扫描 129 (1.104 分): 16091325.D\data.ms
m/z-->
OCH3
S
N
208
165
343
312
236
195
298
152
273
328
109
69
139
177
82
89
39
51
15
29
101
116
126
188
219
226
254
264
284
319

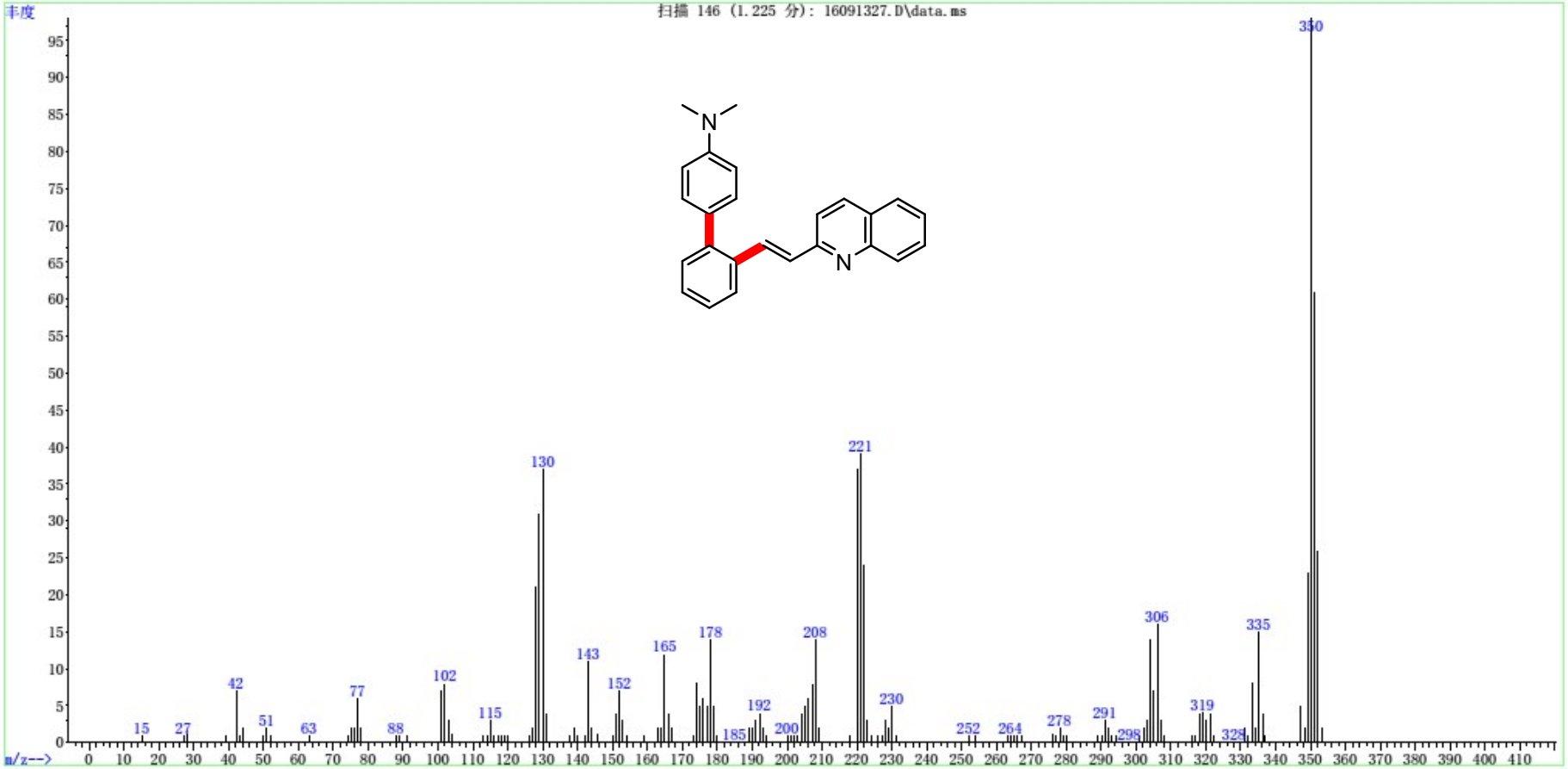
丰度
扫描 146 (1.225 分): 16091327.D\data.ms
N
N
m/z-->
350
221
130
306
335
208
178
165
143
102
152
77
42
230
319
192
115
291
278
51
27
15
63
88
200
252
264
298
329
185

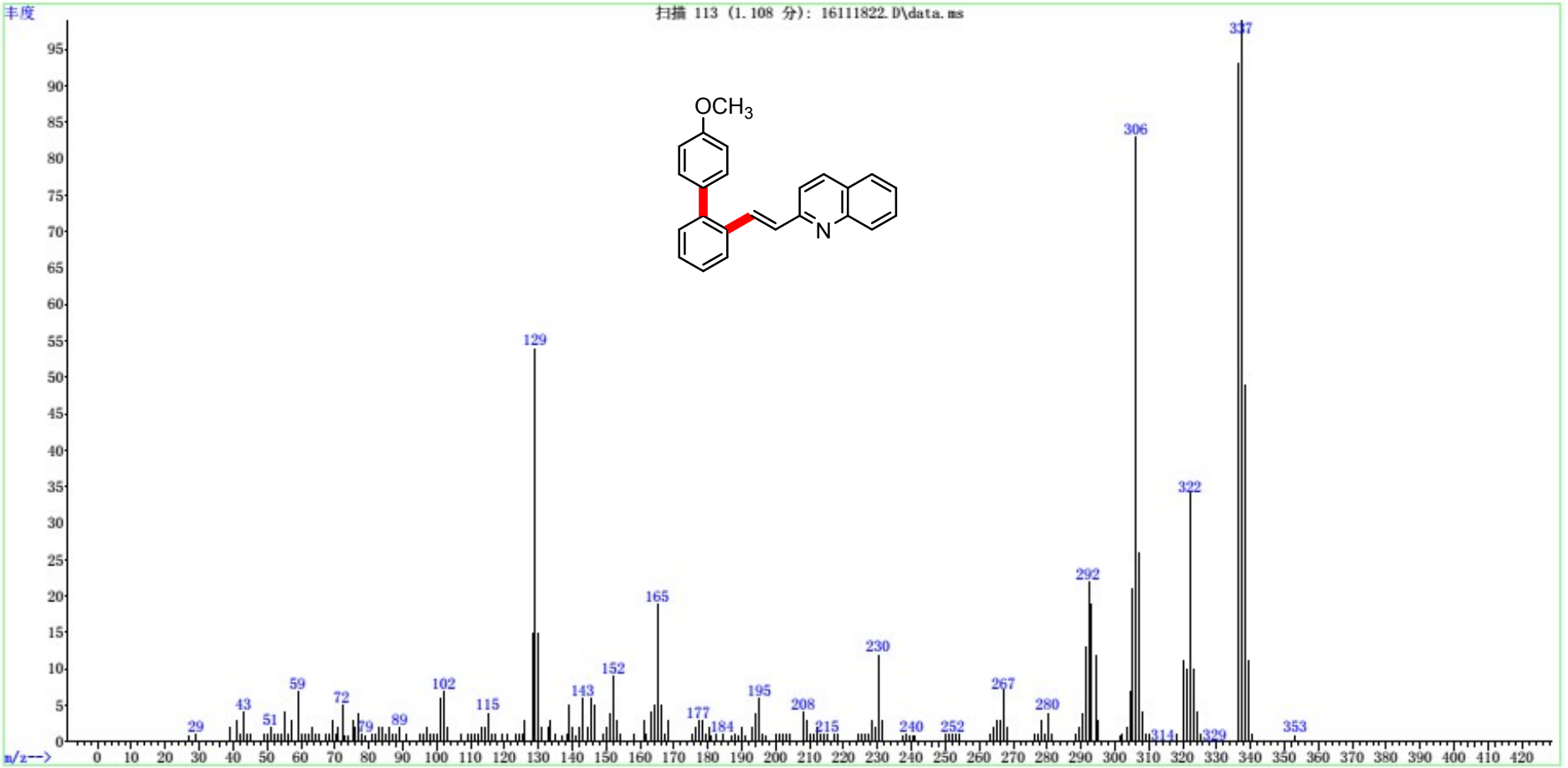
丰度
扫描 113 (1.108 分): 16111822.D\data.ms
OCH3
N
m/z-->
337
306
322
292
129
165
230
152
143
102
59
72
43
51
29
89
115
195
208
267
280
177
184
215
240
252
314
329
353

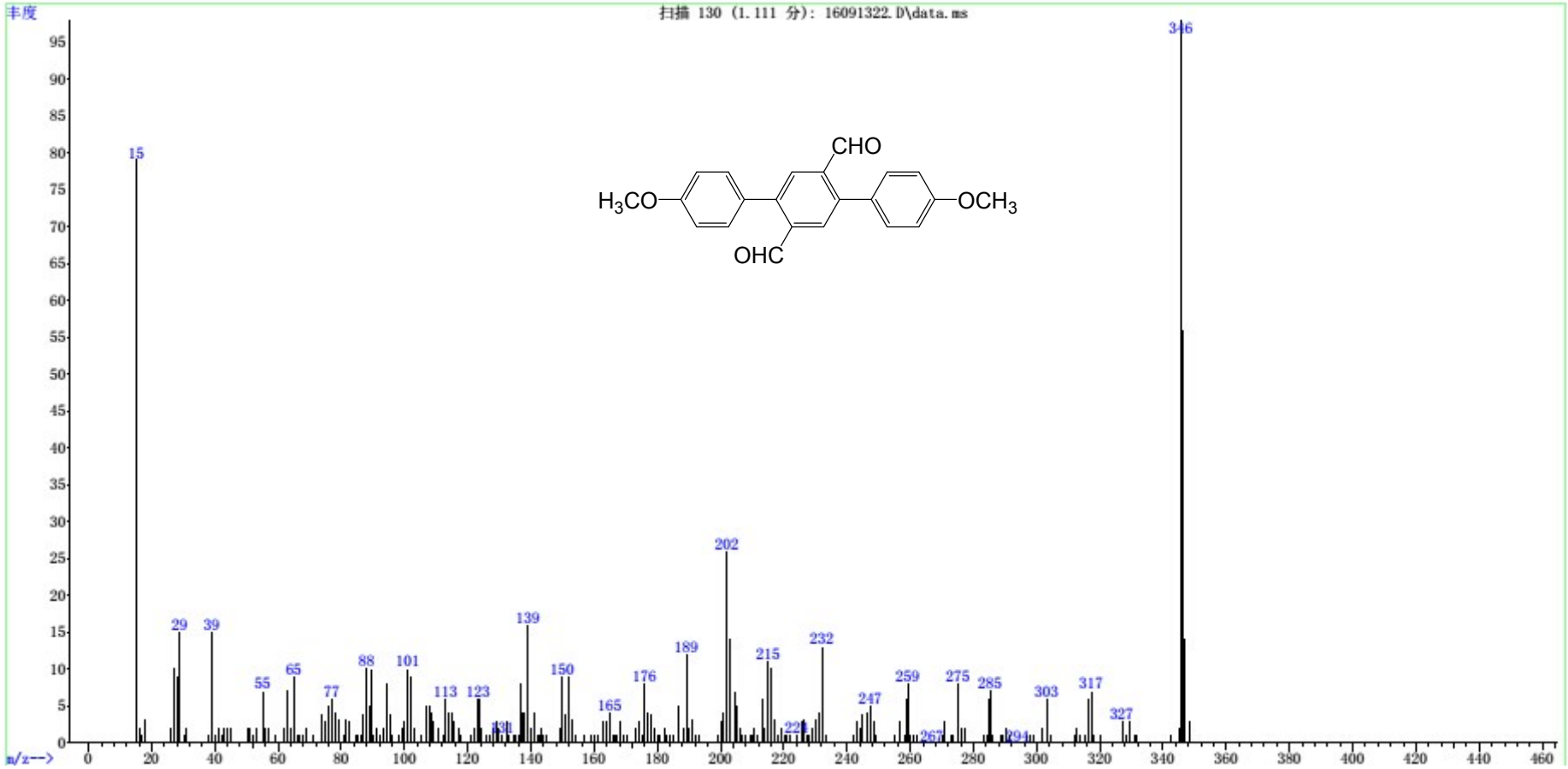
丰度
扫描 130 (1.111 分): 16091322.D\data.ms
m/z-->
CHO
OHC
H3CO
OCH3
346
15
202
29
39
139
232
189
215
55
65
88
101
150
176
259
275
285
303
317
247
77
113
123
165
327

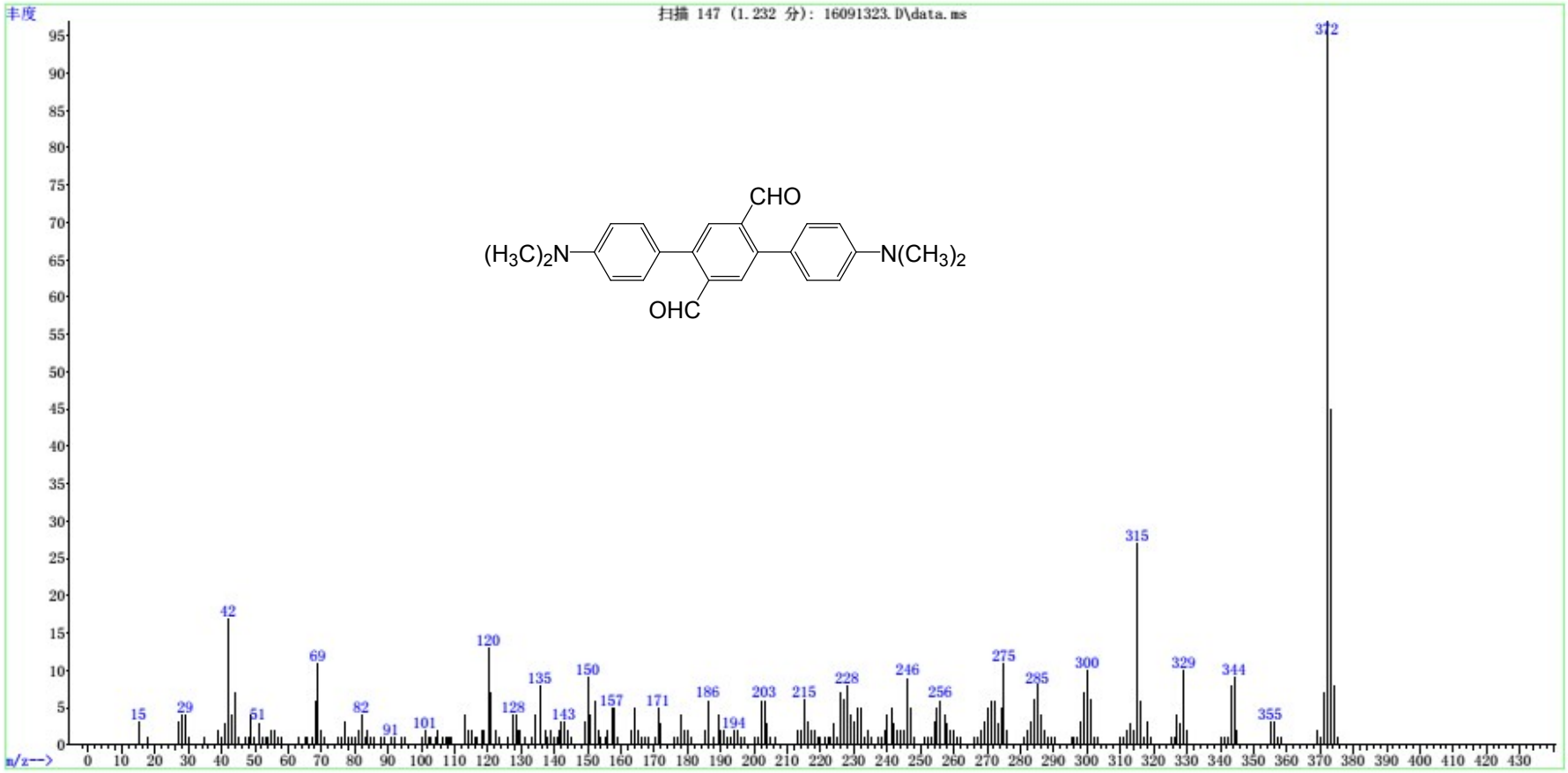
丰度
扫描 147 (1.232 分): 16091323.D\data.ms
CHO
(H3C)2N
N(CH3)2
OHC
m/z-->
372
315
42
69
120
135
150
246
275
285
300
329
344
355
15
29
51
82
91
101
128
143
157
171
186
194
203
215
228
256

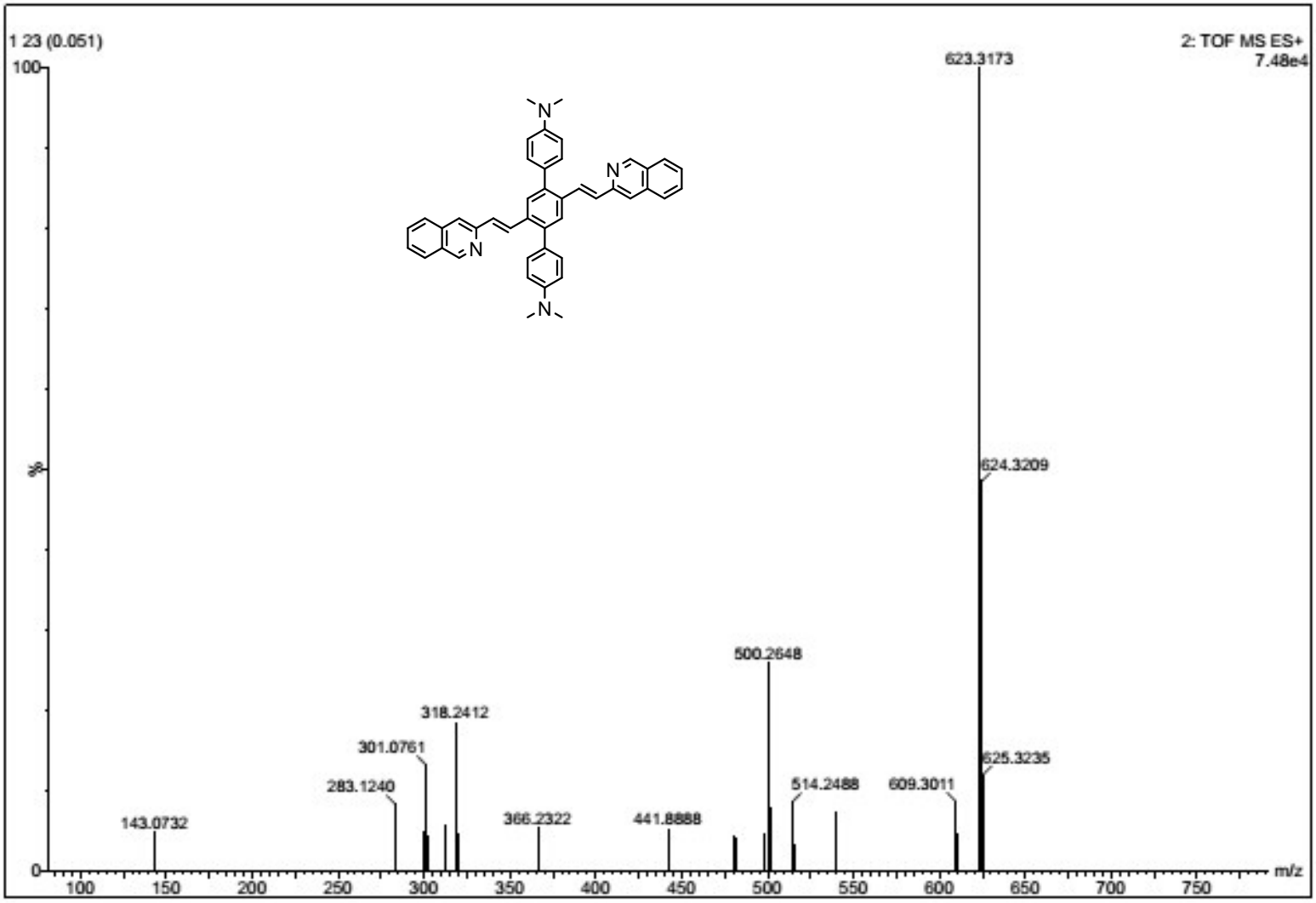
1 23 (0.051)
2: TOF MS ES+
7.48e4
100
%
0
623.3173
624.3209
625.3235
500.2648
318.2412
301.0761
283.1240
143.0732
366.2322
441.8888
514.2488
609.3011
m/z
100
150
200
250
300
350
400
450
500
550
600
650
700
750

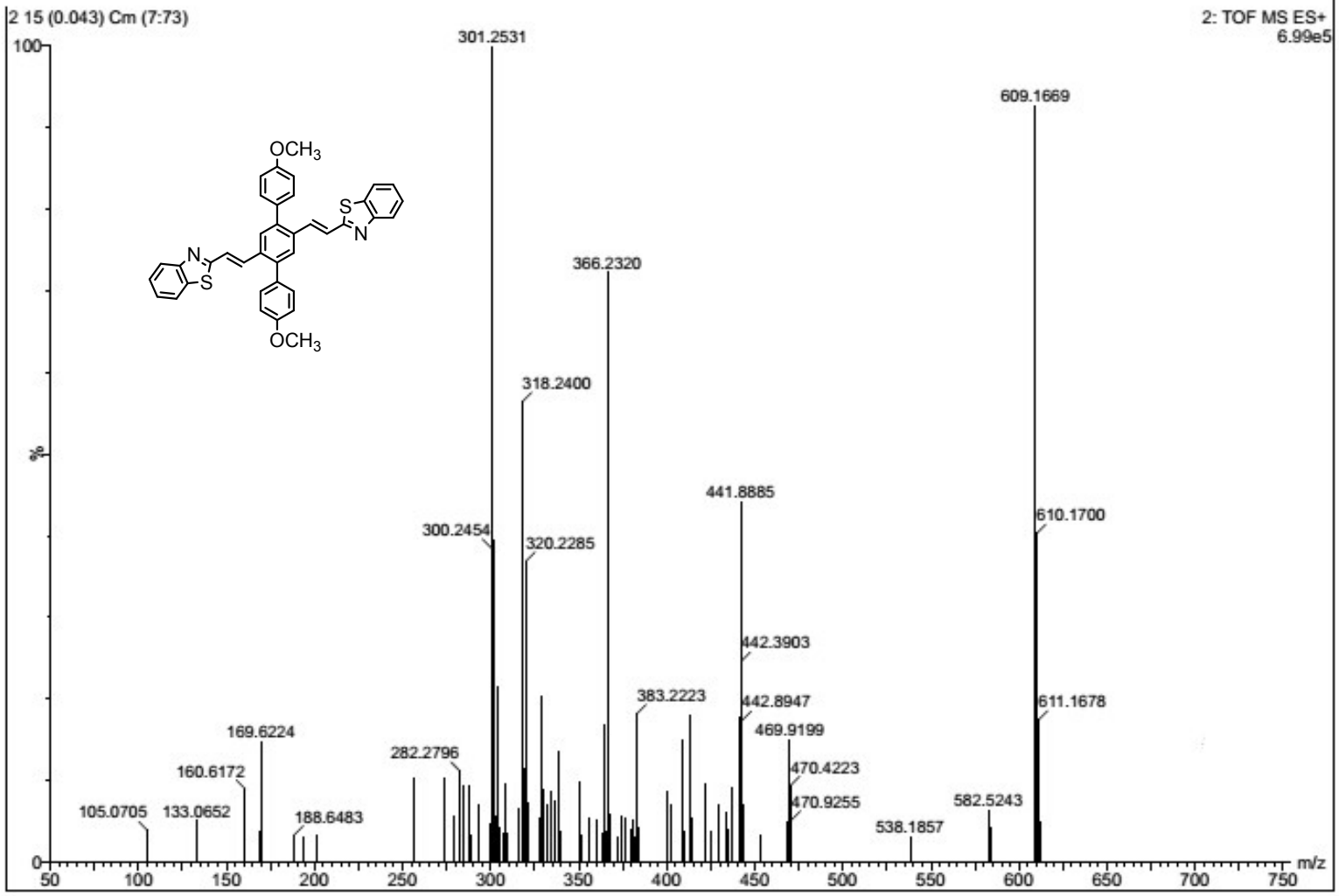
2 15 (0.043) Cm (7:73)
2: TOF MS ES+
6.99e5
100
%
0
301.2531
609.1669
366.2320
318.2400
441.8885
610.1700
300.2454
320.2285
442.3903
383.2223
442.8947
611.1678
469.9199
169.6224
282.2796
160.6172
470.4223
470.9255
582.5243
105.0705
133.0652
188.6483
538.1857
m/z
50
100
150
200
250
300
350
400
450
500
550
600
650
700
750
OCH3
OCH3
N
S
S
N